FINNISH METEOROLOGICAL INSTITUTE
CONTRIBUTIONS

No. 122

TRANSPORTS AND WATER MASSES IN THE FRAM STRAIT AND ITS VICINITY FROM THREE DECADES OF HYDROGRAPHIC OBSERVATIONS IN 1980-2010

Marika Marnela

Department of Physics
Faculty of Science
University of Helsinki
Helsinki, Finland

ACADEMIC DISSERTATION in geophysics

To be presented, with the permission of the Faculty of Science of the University of Helsinki, for public criticism in Auditorium Physicum D101 (Gustaf Hällströminkatu 2 A, Helsinki) on 30th September 2016, at 12 o'clock noon.

Finnish Meteorological Institute
Helsinki, 2016

ISBN 978-951-697-888-1 (paperback)
ISSN 0782-6117
Erweko
Helsinki 2016

ISBN 978-951-697-889-8 (pdf)
http://ethesis.helsinki.fi
Helsinki 2016
Helsingin yliopiston verkkojulkaisut

To Bamsse and Bettina

FINNISH METEOROLOGICAL INSTITUTE

Published by Finnish Meteorological Institute
(Erik Palménin aukio 1), P.O. Box 503
FIN-00101 Helsinki, Finland

Series title, number and report code of publication
Finnish Meteorological Institute
Contributions 122, FMI-CONT-122

Date
July 2016

Author
Marika Marnela

Title
Transports and water masses in the Fram Strait and its vicinity from three decades of hydrographic observations in 1980-2010

Abstract

The Arctic Ocean and its exchanges with the Nordic Seas influence the north-European climate. The Fram Strait with its 2600 m sill depth is the only deep passage between the Arctic Ocean and the other oceans. Not just all the deep water exchanges between the Arctic Ocean and the rest of the world's oceans take place through the Fram Strait, but also a significant amount of cold, low-saline surface waters and sea ice exit the Arctic Ocean through the strait. Correspondingly, part of the warm and saline Atlantic water flowing northward enters the Arctic Ocean through the Fram Strait bringing heat into the Arctic Ocean.

The oceanic exchanges through the Fram Strait as well as the water mass properties and the changes they undergo in the Fram Strait and its vicinity are studied from three decades of ship-based hydrographic observations collected from 1980-2010. The transports are estimated from geostrophic velocities. The main section, comprised of hydrographic stations, is located zonally at about 79 °N. For a few years of the observed period it is possible to combine the 79 °N section with a more northern section, or with a meridional section at the Greenwich meridian, to form quasi-closed boxes and to apply conservation constraints on them in order to estimate the transports through the Fram strait as well as the recirculation in the strait. In a similar way, zonal hydrographic sections in the Fram Strait and along 75 °N crossing the Greenland Sea are combined to study the exchanges between the Nordic Seas and the Fram Strait. The transport estimates are adjusted with drift estimates based on Argo floats in the Greenland Sea. The mean net volume transports through the Fram Strait are averaged from the various approaches and range from less than 1 Sv to about 3 Sv.

The heat loss to the atmosphere from the quasi-closed boxes both north and south of the Fram Strait section is estimated at about 10 TW. The net freshwater transport through the Fram Strait is estimated at 60-70 mSv southward.

The insufficiently known northward transport of Arctic Intermediate Water (AIW) originating in the Nordic Seas is estimated using 2002 Oden expedition data. At the time of data collection, excess sulphur hexafluoride (SF_6) was available, a tracer that besides a background anthropogenic origin derives from a mixing experiment in the Greenland Sea in 1996. The excess SF_6 can be used to distinguish AIW from the upper Polar Deep Water originating in the Arctic Ocean. It is estimated that 0.5 Sv of AIW enters the Arctic Ocean.

The deep waters in the Nordic Seas and in the Arctic Ocean have become warmer and in the Greenland Sea also more saline during the three decades studied in this work. The temperature and salinity properties of the deep waters found in the Fram Strait from both Arctic Ocean and Greenland Sea origins have become similar and continue to do so. How these changes will affect the circulation patterns will be seen in the future.

Publishing unit
Finnish Meteorological Institute, Marine Research Unit

Classification (UDC)
551.463
551.465
551.46

Keywords
Fram Strait, Nordic Seas, geostrophy, transports, recirculation, water mass

ISSN and series title
0782-6117 Finnish Meteorological Institute Contributions

ISBN	Language	Pages
978-951-697-888-1	English	178

ILMATIETEEN LAITOS

Julkaisija Ilmatieteen laitos, (Erik Palménin aukio 1)
PL 503, 00101 Helsinki

Julkaisun sarja, numero ja raporttikoodi
Finnish Meteorological Institute
Contributions 122, FMI-CONT-122

Julkaisuaika
Heinäkuu 2016

Tekijä
Marika Marnela

Nimeke
Kuljetukset ja vesimassat Framin salmessa ja sen läheisyydessä perustuen 30-vuotiseen hydrografiseen havaintoaineistoon 1980-2010

Tiivistelmä

Pohjoinen jäämeri sekä sen vuorovaikutukset Luoteis-Euroopan merien kanssa vaikuttavat Pohjois-Euroopan ilmastoon. Framin salmi 2600 m kynnyssyvyydellään on Pohjoisen jäämeren ainoa syvä yhteys muihin maailman meriin. Syvien vesien vaihdon lisäksi Framin salmen kautta kulkeutuu Pohjoiselta jäämereltä Luoteis-Euroopan meriin huomattava määrä kylmää ja vähäsuolaista pintavettä sekä merijäätä. Framin salmen kautta virtaa myös osa pohjoiseen kulkeutuvasta lämpimästä ja suolaisesta Atlantin vedestä tuoden lämpöä Pohjoiselle jäämerelle.

Tutkimuksessa tarkastellaan Framin salmen vedenvaihtoa ja Framin salmessa sekä sen läheisyydessä tavattavien vesimassojen ominaisuuksia ja vesimassoissa havaittuja muutoksia. Hydrografinen havaintoaineisto on kerätty laivoilta käsin kolmen vuosikymmenen aikana, vuosina 1980-2010. Kuljetukset arvioidaan laskettujen geostrofisten nopeuksien perusteella. Tutkimuksen tärkein hydrografisista luotausasemista muodostuva poikkileikkaus kulkee Framin salmen poikki noin pitkin 79° pohjoista leveyspiiriä. Muutamana vuonna havaintojakson aikana on mahdollista arvioida Framin salmen kuljetuksia ja Atlantin veden resirkulaatiota eli kiertämistä salmessa takaisin etelään yhdistämällä Framin salmen poikkileikkaus pohjoisemman itä-länsisuuntaisen poikkileikkauksen tai Greenwichin meridiaania pitkin kulkevan poikkileikkauksen kanssa ja vaatimalla tasapaino poikkileikkausten välisille kuljetuksille. Samoin tutkimuksessa arvioidaan kuljetuksia Framin salmen ja Luoteis-Euroopan merien välillä yhdistämällä hydrografinen poikkileikkaus Framin salmessa toiseen, pitkin 75 ° pohjoista leveyspiiriä kulkevaan ja Grönlanninmeren ylittävään poikkileikkaukseen. Kuljetusarviota muokataan Grönlanninmerellä ajelehtivien Argo-poijujen liikkeen perusteella. Tutkimuksessa käytettävillä menetelmillä arvioidaan Framin salmen nettotilavuuskuljetusten olevan keskimäärin alle yhdestä Sv noin kolmeen Sv etelään.

Tutkimuksessa arvioidaan, että lämmön menetys ilmakehään kahden poikkileikkauksen väliseltä alueelta sekä pohjoiseen että etelään Framin salmesta on noin 10 TW. Makean veden nettokuljetuksen Framin salmen kautta arvioidaan olevan 60-70 mSv etelään.

Luoteis-Euroopan merillä muodostuvan Arktisen keskisyvän vesimassan (AIW) kuljetus pohjoiseen tunnetaan huonosti. Tutkimuksessa AIW voidaan erottaa vuoden 2002 havaintoaineistosta Pohjoisella jäämerellä muodostuvasta keskisyvästä vesimassasta hyödyntäen vuoden 1996 Grönlanninmeren sekoittumiskokeesta peräisin olevaa rikkiheksafluoridia. Tutkimuksessa arvioidaan, että 0.5 Sv AIW:ta kulkeutuu Pohjoiselle jäämerelle.

Syvät vedet ovat lämmenneet sekä Pohjoiella jäämerellä että Luoteis-Euroopan merillä ja Grönlanninmerellä myös suolaistuneet tutkimuksessa havainnoidun kolmen vuosikymmenen aikana. Framin salmessa tavataan sekä jäämereltä että Grönlanninmereltä peräisin olevia syviä vesiä. Niiden ominaisuudet (lämpötila ja suolaisuus) ovat samankaltaistuneet ja samankaltaistuvat edelleen. Havaittujen muutosten vaikutukset merien kiertoliikkeeseen selviävät tulevaisuudessa.

Julkaisijayksikkö
Ilmatieteen laitos, Merentutkimus

Luokitus (UDK)
551.463
551.465
551.46

Asiasanat
Framin salmi, Luoteis-Euroopan meret,
geostrofia, kuljetukset, resirkulaatio, vesimassa

ISSN ja avainnimike
0782-6117 Finnish Meteorological Institute Contributions

ISBN	Kieli	Sivumäärä
978-951-697-888-1	Englanti	178

Contents

List of original publications

The thesis is based on the following papers which are referred to in the text by their Roman numerals:

I Rudels, B., M. Marnela, and P. Eriksson (2008), Constraints on estimating mass, heat and freshwater transports in the Arctic Ocean: An exercise, In: Dickson, R. R., J. Meincke and P. Rhines (Eds.) Arctic-Subarctic Ocean Fluxes, Springer, Dordrecht, 315-341.

II Marnela, M., B. Rudels, K. A. Olsson, L. G. Anderson, E. Jeansson, D. Torres, M.-J. Messias, J. H. Swift, and A. J. Watson (2008), Transports of Nordic Seas water masses and excess SF_6 through Fram Strait to the Arctic Ocean, Progress in Oceanography, 78 (1), 1-11, doi:10.1016/j.pocean.2007.06.004.

III Marnela, M., B. Rudels, and P. B. Eriksson (2009), Finnish studies of physical Arctic oceanography, Geophysica, 45 (1-2), 147-162.

IV Marnela, M., B. Rudels, M.-N. Houssais, A. Beszczynska-Möller, and P. B. Eriksson (2013), Recirculation in the Fram Strait and transports of water in and north of the Fram Strait derived from CTD data, Ocean Science, 9, 499-519, doi:10.5194/os-9-499-2013.

V Marnela, M., B. Rudels, I. Goszczko, A. Beszczynska-Möller, and U. Schauer (2016), Fram Strait and Greenland Sea transports, water masses and water mass transformations 1999-2010 (and beyond). Journal of Geophysical Research, Oceans, 121, 2314-2346, doi:10.1002/2015JC011312.

Author's contribution

I = mostly responsible for, II = largely responsible for, III = partly responsible for.

	Paper I	Paper II	Paper III	Paper IV	Paper V
Data analysis and computations	II	I*	II	I	I
Writing		II	I	I	I
Field work [years]	2003, 2004		2002-2005, 2008	2003, 2004	2003, 2004, 2006, 2008

* Except tracer and lADCP analysis.

Field work consists of participation on cruises. The years presented in the table correspond to research vessels and study areas as follows: 2002 Finnish Marine Research Institute's (now Finnish Environment Institute's) RV Aranda in the Fram Strait, 2003 Norwegian Polar Institute's RV Lance in the Fram Strait, 2004 German Alfred Wegener Institute's RV Polarstern in and north of the Fram Strait, 2005 Icelandic Marine Research Institute's RV Árni Friðriksson in the Denmark Strait, 2006 German Leibniz Institute for Baltic Sea Research's RV Maria S. Merian in the Greenland Sea, 2008 Polar Research Institute of China's MV XueLong in the Arctic Ocean.

1 Introduction

The cold and remote Arctic has continued to be an inspiring subject of oceanographic studies for over a century. Nansen's expedition with the ship Fram during 1893-1896 produced observational data about the waters in the Arctic Ocean (Nansen, 1902). Russian / Soviet floating ice stations have collected data inside the Arctic Ocean year-round since 1937 (Treshnikov et al., 1977). Later generations of oceanographers have continued to make observations, adding details and making corrections to circulation schemes of the Arctic Mediterranean (i.e. the Arctic Ocean and Greenland, Iceland and Norwegian Seas; **Fig. 1**) (e.g. Worthington, 1953; Coachman and Barnes, 1963; Aagaard, 1981; Rudels et al., 1994; Proshutinsky et al., 2015), and documented changes in the water mass properties (e.g. Aagaard et al., 1985; Schlichtholz and Houssais, 2002; Rudels et al, 2013; Somavilla et al., 2013). Models are used to compensate for the spatially and temporally sparse observational data and to help understand the past and present processes and changes with an aim to predicting the future (e.g. Karcher et al., 2012; Spall, 2013; Nummelin et al., 2015).

Climate change has increased the interest in the Arctic Ocean, not just from a scientific point of view but also from an economic one. A northern sea-route could be utilized, and natural resources exploited, in a less ice-covered Arctic. In societal terms, predictions of future environmental changes are of great assistance in preparing for change, or for trying to mitigate the changes through political decision-making. In order to predict the future, the present system needs to be understood. The oceans act as a buffer for the changes in the concentration of the greenhouse gas carbon dioxide (e.g. Tanhua et al., 2009), but their buffering capacity has limits and the oceans are at the same time undergoing changes, e.g. acidifying (Orr et al., 2005). Another important greenhouse gas methane is being released from the subsea permafrost in the warming Arctic shelves (Shakhova et al., 2014). The Arctic Ocean sea ice has been observed to have declined in the past few decades in its coverage, thickness and volume (Kwok et al., 2009; Stroeve et al., 2014). As the highly reflective sea ice and snow cover is diminishing and more dark ocean surface is exposed, more sunlight is absorbed, warming the surface waters and amplifying the warming effect further (e.g. Holland et al., 2012). The Arctic Ocean is predicted to be nearly ice-free during summertime within the next couple of decades (Overland and Wang, 2013). Understanding how the Arctic Ocean and its sensitive ecosystems function, from planktonic scales (Arrigo et al., 2008) to marine mammals (e.g. Bromaghin et al., 2015), will help to minimize the damages inflicted on them by human activity in a changing Arctic environment. An improved understanding of the Arctic Ocean is also important from a commercial point of view for e.g. helping to secure safe navigation and operations (Stephenson et al., 2013).

The Arctic Ocean and the thermohaline circulation influence the north-European climate (Serreze et al., 2006; Srokosz et al., 2012). The thermohaline circulation brings warm and saline waters from lower latitudes, where the high salinity is created by evaporation exceeding precipitation, to higher latitudes. The waters cool and due to their increasing density then sink, mix, and return southward along the ocean floor, ventilating and renewing the deep waters of the oceans (Rahmstorf, 2006; Dickson et al., 2008). About 7.4 ± 1.1 Sv (1 Sv = 10^6 m^3/s) of the saline and warm Atlantic Water (AW) flow north-eastward and enter the Nordic Seas (Greenland, Iceland and Norwegian seas) across the Greenland-Scotland Ridge with a maximum sill depth of

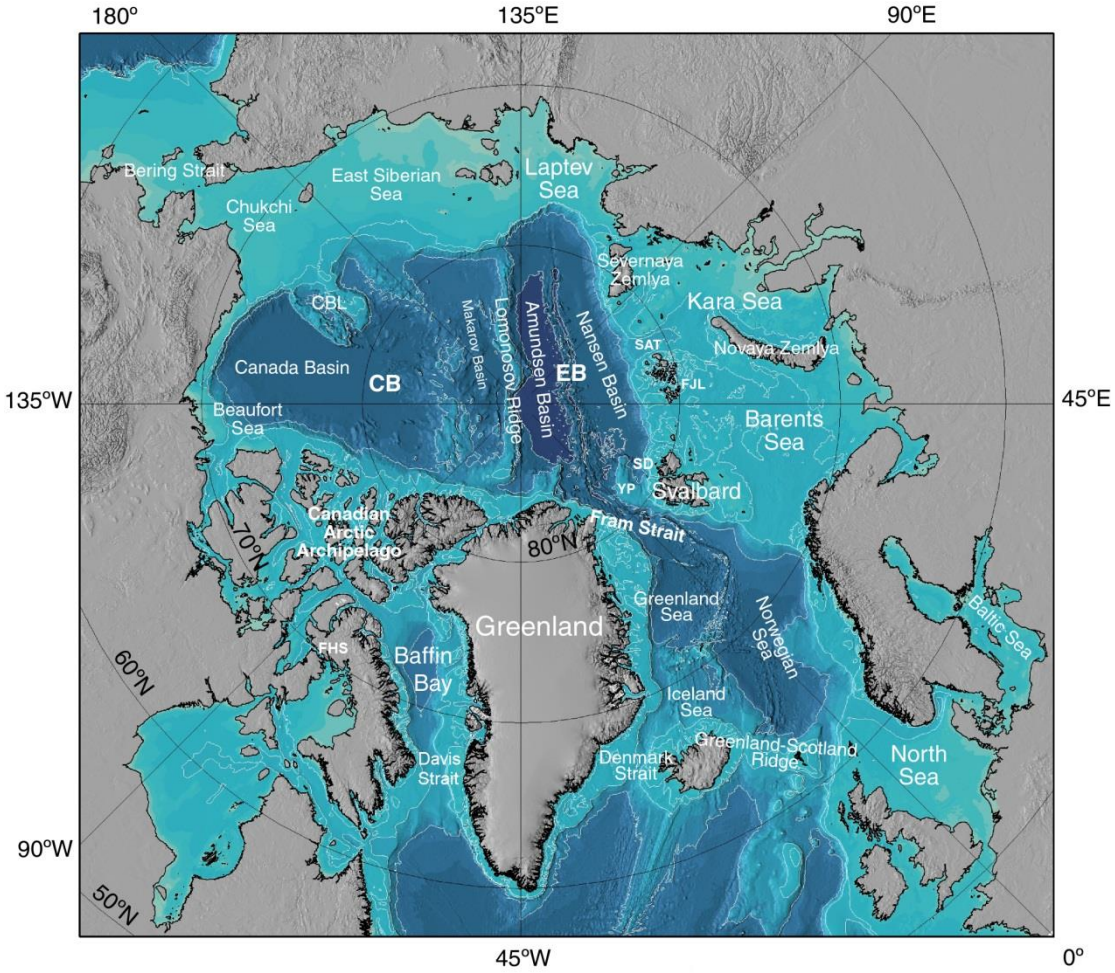

Figure 1: Bathymetric map of the Arctic Ocean and the Nordic Seas. See list of Abbreviations for the description of the acronyms. Modified from paper III, originally adapted from Encyclopedia of Ocean Sciences, 2nd ed., 2008.

slightly over 800 m, with some additional flow over continental shelf areas (Jónsson and Valdimarsson, 2012; Berx et al., 2013; Hansen et al., 2015) (**Fig.2**). Part of the AW takes part in the formation of Arctic Intermediate water (AIW) in the Nordic Seas through convection (e.g. Swift and Aagaard, 1981), and leaves the Nordic Seas as dense overflow waters (Dickson et al., 2008); a part enters the Arctic Ocean through the Barents Sea (e.g. Ingvaldsen et al., 2004) and the Fram Strait (e.g. Rudels, 1987), and a further part of AW recirculates in the Fram Strait (e.g. Bourke et al., 1988; Manley, 1995).

The Fram Strait branch of AW that continues into the Arctic Ocean loses a large amount of heat just north of Svalbard, in an area called Whaler's Bay (Wiig et al., 2007), to ice melt and to the atmosphere (Rudels et al., 1999; Tetzlaff et al., 2014) and continues along the continental slope to the east. The Barents Sea branch is cooled and freshened in the Barents Sea and enters the deep Arctic Ocean via the St. Anna Trough north of the Kara Sea (Rudels et al., 1994; Dmitrenko et al., 2015). Both branches circulate the Arctic Ocean basins anticlockwise (Rudels et al., 1999). The surface waters in the Arctic Ocean have low salinity, from about 24 to 34 psu, due to ice melt, river runoff and Pacific inflow (e.g. Rudels et al., 1996). The upper part of AW is diluted by ice melt and cooled in the Nansen Basin to freezing temperature. It becomes the Arctic Ocean lower halocline water at about 200 m depth as it continues eastward and is

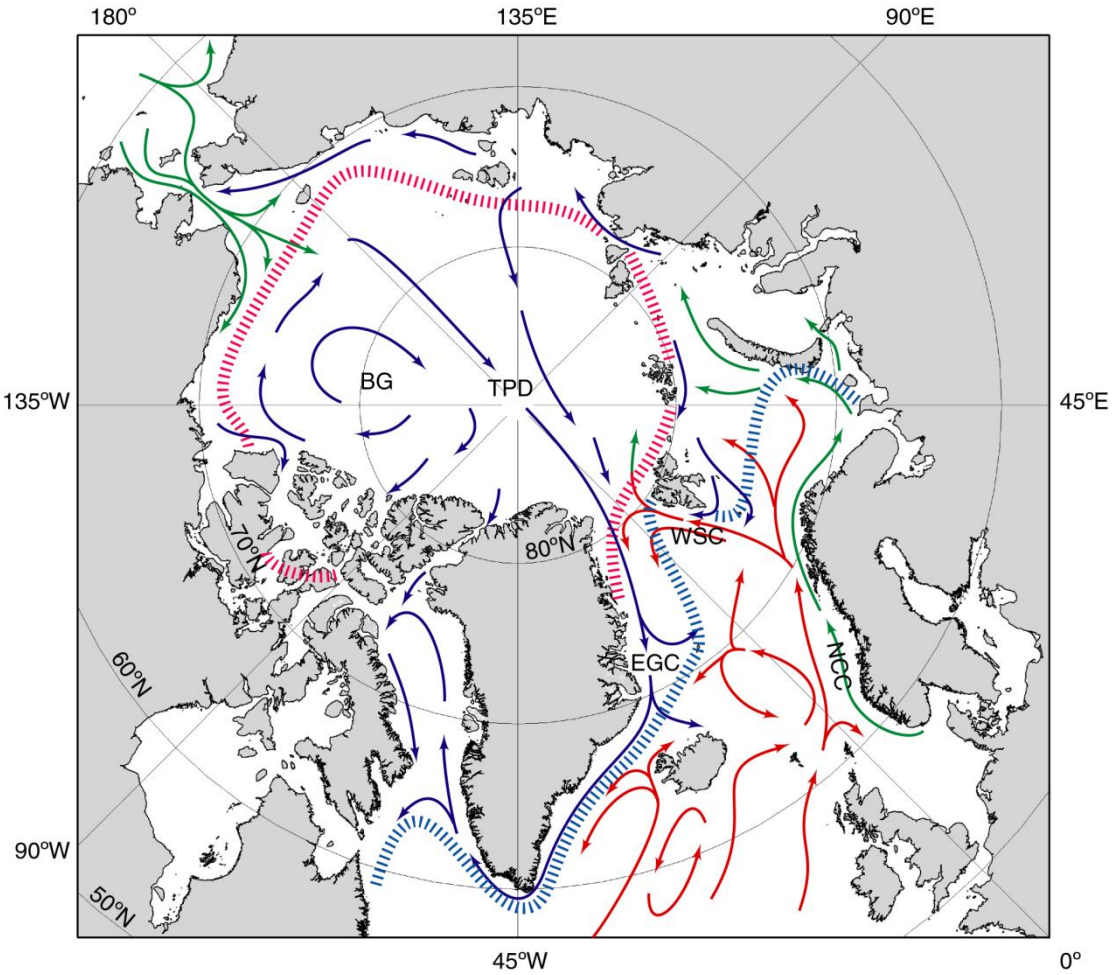

Figure 2: Arctic Ocean and Nordic Seas surface circulation. See list of Abbreviations for the description of the acronyms. From paper III, originally adapted from Encyclopedia of Ocean Sciences, 2nd ed., 2008.

overrun by less dense shelf water (Rudels 1996; Karcher and Oberhuber, 2002; Rudels et al., 2004; 2005) (**Fig. 3**). The Arctic Ocean upper halocline is formed by Pacific waters (Jones and Anderson, 1986). Part of the AW recirculates in the Nansen and Amundsen basins and a smaller part continues along the continental slope into the Canadian basin (Rudels et al., 2001; 2013). The Fram Strait branch is mostly limited to the Nansen Basin (Rudels et al., 2013). In the Canadian Basin the warm and saline AW is still seen in the temperature and salinity diagrams (θS diagrams) as a temperature maximum, with the lower halocline water originating in the Nansen Basin as a temperature minimum above it and intermediate water originating from the Barents Sea as a cold and fresh layer below it **(Fig. 4,** from paper III, Fig. 7). The Arctic Ocean deep waters are modified slowly and take 200-300 years to ventilate (Tanhua et al., 2009).

The exchanges between the Arctic Ocean and the rest of the oceans take place through: the Bering Strait, with a flow into the Arctic Ocean of 0.4-1.2 Sv (1 Sv = 10^6 m^3/s) of strong seasonal variability (Woodgate et al., 2005) and an increasing trend of 0.03 ± 0.2 Sv / year (Woodgate et al., 2012); the Canadian Arctic Archipelago (CAA), with a net export out of the Arctic estimated as 1.6 ± 0.2 Sv through the Davis Strait and with an additional outflow of about 0.1 Sv through a narrow Fury and Hecla Strait (Curry et al., 2014); the Barents Sea Opening, with 2.3-3.3 Sv into the Arctic (the most recent estimates are from the higher end), of which 0.8-1.8 Sv is estimated to be carried

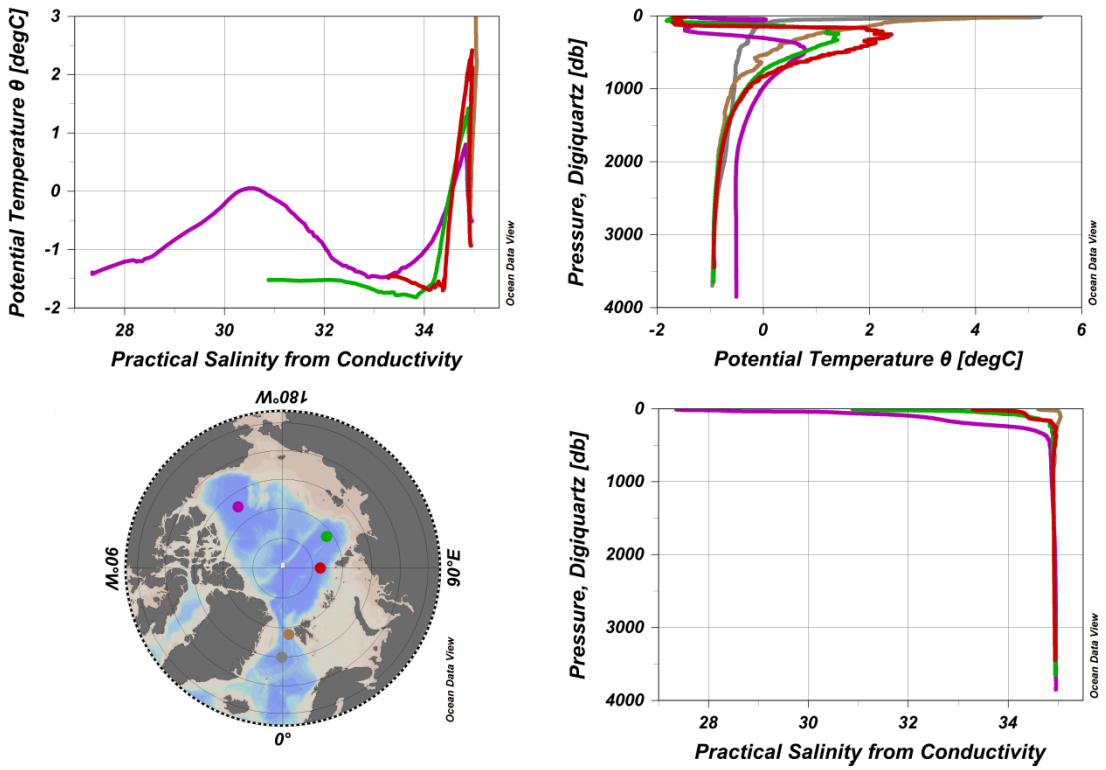

Figure 3. Potential temperature (θ) and salinity (S) profiles and a θS diagram from the Greenland Sea (gray), eastern Fram Strait (brown), and Arctic Ocean: Nansen (red), Amundsen (green) and Canada (purple) basins in 2013.

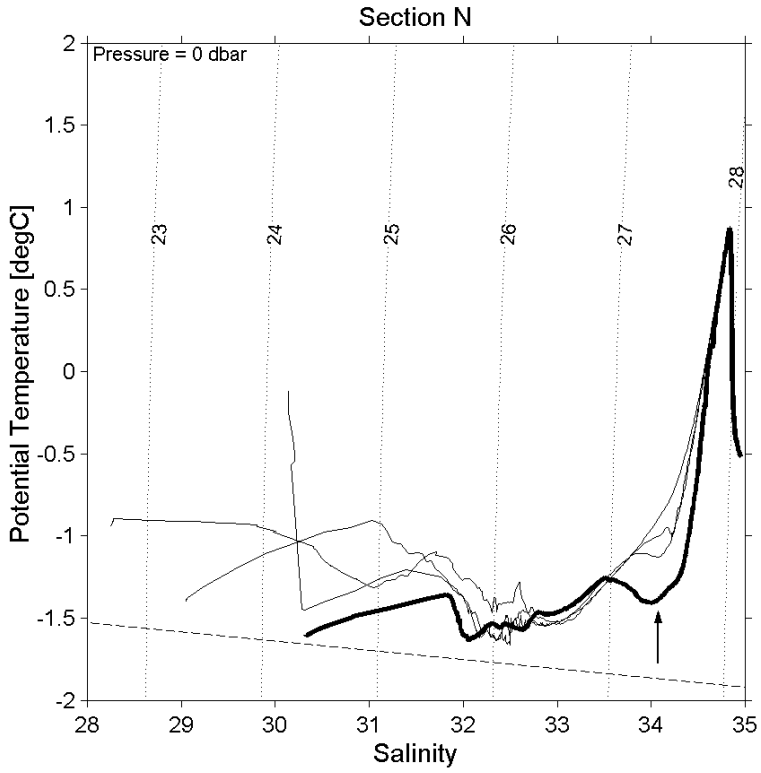

Figure 4: θS diagram of the Chinare 2008 cruise on XueLong section N located on the western side of Chukchi Borderland. The arrow points out the lower halocline water originating from the Nansen Basin. AW is seen as a temperature maximum close to 1 °C. From paper III, Figure 7.

by the Norwegian Coastal Current (NCC) (Skagseth et al., 2011, Smedsrud, et al., 2013; Rudels et al., 2015); and the Fram Strait, with a net flow out of the Arctic (e.g. Fahrbach et al., 2001; Schauer et al., 2004; Fieg et al., 2010), and which is the only deep passage between the Arctic Ocean and the rest of the oceans. When considering the water budget of the Arctic Ocean, river runoff and precipitation minus evaporation need to be taken into account. Serreze et al. (2006) estimated the freshwater input to the Arctic Ocean from the rivers and precipitation at 0.15-0.20 Sv. The amount of meltwater from glaciers inside the Arctic Ocean equals to about 5% of the river runoff and is not significant (Carmack et al., 2015). (**Fig 5**).

Heat transport can be estimated for a region if the mass transport is balanced. Volume or mass transports through a section often are imbalanced, and the estimated heat transport will depend on the temperature scale and becomes arbitrary (e.g. Schauer and Beszczynska-Möller, 2009). The whole Arctic Ocean or all its entrances need to be covered synoptically to be able to estimate the heat transport at any of the entrances. Such an attempt was made by Tsubouchi et al. (2012) from 2005 summer data. They obtained a heat flux for the Arctic Ocean of 189 ± 26 TW (lost to the atmosphere), with close to half carried through the Barents Sea Opening and a quarter through the Fram Strait. The mass transport in the Arctic Ocean transport computations is often not balanced. Heat and freshwater transports have then been estimated relative to a reference temperature and salinity. The often used mean temperature and salinity of the Arctic Ocean, -0.1 °C and 34.80 respectively, have been estimated from rather sparse and early data, but also other more local reference values have been used (e.g. Aagaard and Greisman, 1975; Aagaard and Carmack 1989; Schauer and Beszczynska-Möller, 2009; Rabe et al., 2009; 2013).

This work focuses on the exchanges through the Fram Strait estimated from a geostrophic method, and on the changes in the water masses present. In the Fram Strait a northward flow is present in the east carried by the West Spitsbergen Current (WSC) and a southward flow in the west carried by the East Greenland Current (EGC) (e.g. Aagaard et al., 1973; Foldvik et al., 1988) (**Fig. 2**). The net volume transport in the Fram Strait is southward. Waters with properties from the Arctic Ocean as well as waters with properties from the Nordic Seas are found in the strait. They are modified en route to the Fram Strait, but also interact within the strait (von Appen et al., 2015). Brine rejection due to ice formation causes dense water to cascade over the continental shelves; occasionally such dense and saline water is present in the eastern part of the Fram Strait (Rudels et al., 2005; Skogseth et al., 2005). The bottom features in the Fram Strait are variable, with the deepest parts close to 2600 m, and partly direct the flow (Jakobsson et al., 2012; von Appen et al., 2015). Both baroclinic and barotropic eddies are present in the strait (e.g. Teigen et al., 2011).

Most of the ship-borne observations in the Arctic and sub-Arctic waters are from summer. The volume transport, as well as its variations, has been estimated from a mooring array of current meters in the Fram Strait maintained regularly since 1997, and although a winter maximum has been found in the WSC, no clear trend for the net volume through the whole strait has been found (Fahrbach et al., 2001; Schauer et al., 2004; Schauer and Beszczynska-Möller, 2009; Fieg et al., 2010). However, de Steur et al. (2014) find a seasonal signal in the EGC with summer minimum and winter maximum, as well as a reduction in variability, after the mooring array's location has been altered in 2002 from 79 °N to 78 °50 'N. This seasonality is also reflected in the net volume transport until 2006, but after that gets less clear (see Schauer and Beszczynska-Möller, 2009, Fig. 5).

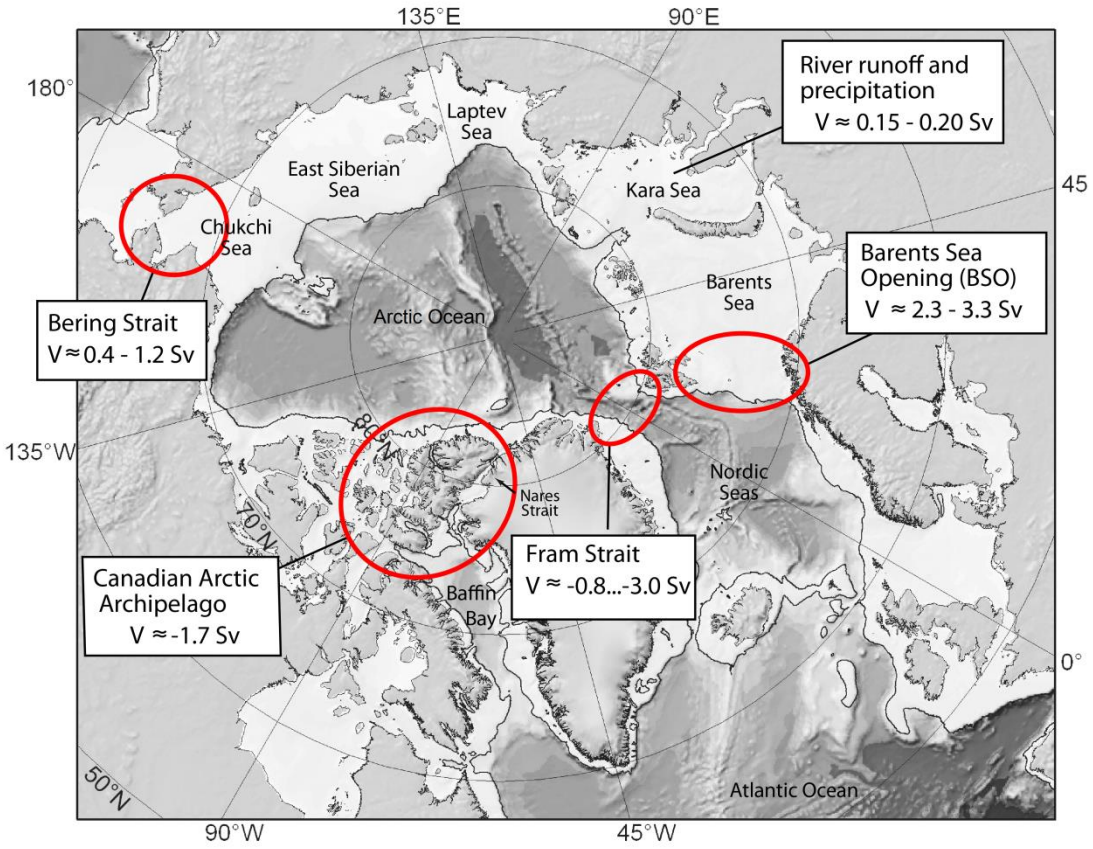

Figure 5: Map of the Arctic Mediterranean with the net volume fluxes at the entrances of the Arctic Ocean. Positive values = net inflow to the Arctic Ocean, negative values = net outflow from the Arctic Ocean. Modified from paper I based on values by various authors presented in the Introduction and Conclusions.

Several estimates have been given for the Fram Strait heat and freshwater transports relative to reference temperatures and salinities. A way of avoiding the problematics involved with this is to form a closed, balanced, box. Often synoptic data are not available for the whole Arctic or its entrances, and a closed box cannot be formed. In this work two smaller closed areas in the vicinity of the Fram Strait are formed and the heat loss from them is then estimated. Ice and freshwater are transported southward through the Fram Strait by less than or about 100 mSv each (e.g. Vinje, 2001; Kwok et al., 2004; Dickson et al., 2007; Rabe et al., 2013; Carmack et al., 2015). Estimates for the liquid freshwater transports are here computed based on the geostrophic method.

2 Goals of the study

The primary goal of this study is to estimate the transports through the Fram Strait from geostrophic computations (**Table 1**). There are other estimates for this, both from observations and models. These values will mostly provide a summertime minimum and add to the ensemble of estimates. The volume transports when put together with estimates made at the other Arctic Ocean entrances, i.e. the Barents Sea Opening, the Bering Strait and the CAA, contribute to the formulation of a volume budget for the Arctic Ocean. In paper V two zonal hydrographic sections, one in the Fram Strait and the other in the Greenland Sea, are combined to study the exchanges between the Nordic Seas and the Arctic Ocean. The transport estimates are adjusted with drift estimates based on Argo floats.

Besides the amount of water transported through the Fram Strait, the water mass properties are also studied. Three decades of observations provide an opportunity to study the changes in the properties. The warming of the deep waters noted by e.g. Budéus et al. (1998) in the Greenland Sea, Langehaug and Falck (2012) in the Fram Strait and Rudels et al. (2013) in the Arctic Ocean is present. The intermediate waters originate from open ocean convection in the Nordic seas (AIW) and from slope convection related to brine release on the shelves inside the Arctic Ocean (upper Polar Deep Water, uPDW). The intermediate waters of the two origins present in the Fram Strait are distinguished in paper II using the excess amount of transient tracer sulphur hexafluoride (SF_6), and their proportions are estimated for 2002.

Not all of the northward flow in the Fram Strait continues into the Arctic Ocean, but a part of it recirculates south-westward. Estimates for the amount of AW recirculation exist from the 1980s, but an update to those estimates from newer data is in order considering the changes in the water mass properties and possibly also in the circulation.

A significant amount of the oceanic heat transport into the Arctic Ocean is carried by the AW (e.g. Rudels, 1987). An attempt is made in paper I to estimate the heat flux through the Fram Strait relative to the annually varying mean temperature of the southward flow (flow out of the Arctic Ocean). This choice would then give the largest transport of heat through the strait as the cold outflow is larger than the warmer inflow to the Arctic Ocean. Without balancing the other entrances to the Arctic Ocean the results are still rather arbitrary. Another goal is therefore set to estimate the heat loss north of the Fram Strait (paper IV) and later in paper V inside a quasi-closed area between the Fram Strait and the Greenland Sea that can be computed without the results affected by the choice of a reference temperature.

The amount of freshwater, in liquid form, leaving the Arctic Ocean through the Fram Strait is also estimated. It is less sensitive to the choice of reference salinity than the heat transport to reference temperature and a net transport (southward) of freshwater can be estimated as well as the gain / loss inside an area bound by two hydrographic sections and slopes to the east and west.

Table 1: Goals of the study. FS = Fram Strait, GS = Greenland Sea.

Goal \ Estimated in	Paper I	Paper II	Paper III	Paper IV	Paper V
Volume transports from geostrophy	Single section in FS	Single section north of FS	Single sections in FS and double in and north of FS	Double sections in and north of FS	Double sections in FS and GS
Water mass properties and volume transports	Whole water column	Whole water column with focus on intermediate waters	Mostly intermediate waters	Whole water column with focus on AW	Whole water column
Recirculation	Not computed	Not directly computed	Not discussed	Computed from meridional and zonal sections	Not Computed
Heat and freshwater transports	Relative to varying reference values	Not computed	For a quasi-closed area	For a quasi-closed area	For a quasi-closed area

3 Theory

3.1 Forces and motions in the ocean

According to Newton's second law of motion a non-zero external force acting on a system changes the motion of the system directly proportionally to the force and in its direction

$$F = ma \tag{1}$$

where F is the force, m is mass and a is acceleration.

Forces in the ocean can be divided in two classes, ones that cause motion, and ones that result from motion. The primary forces causing motion in the ocean are gravitation, wind stress (tangential i.e. friction, or normal i.e. pressure), atmospheric pressure, and seismic. The secondary forces resulting from motion are the Coriolis force and friction. The Coriolis force is an apparent force caused by Earth's rotation, which acts perpendicular to the velocity of a moving body on the surface of the Earth (Pond and Pickard, 1983). The forces per unit mass thus giving the acceleration term a can be written as an equation of motion (e.g. Pond and Pickard, 1983)

$$a = -\frac{1}{\rho}\nabla p - 2\Omega \times V + g + F_o \tag{2}$$

where ρ is density, p is pressure, Ω is the angular velocity of the Earth ($7.292 \cdot 10^{-5}$ rad/s), V is velocity, g is acceleration due to gravity (about 9.8 m/s^2) and F_o are the other forces present. Pond and Pickard (1983) also present equation (2) written for x (eastward), y (northward), and z (vertical, negative downward) terms

$$\begin{aligned}
\frac{du}{dt} &= -\frac{1}{\rho}\frac{\partial p}{\partial x} + v \cdot 2\Omega \sin\varphi - w \cdot 2\Omega \cos\varphi + F_x \\
\frac{dv}{dt} &= -\frac{1}{\rho}\frac{\partial p}{\partial y} - u \cdot 2\Omega \sin\varphi + F_y \\
\frac{dw}{dt} &= -\frac{1}{\rho}\frac{\partial p}{\partial z} + u \cdot 2\Omega \cos\varphi - g + F_z
\end{aligned} \tag{3}$$

where u and v are the horizontal, and w the vertical velocity components, and φ is latitude.

3.2 Geostrophic currents

The word geostrophic derives from Greek, meaning 'earth turned'. Geostrophic currents result from the balance in the water mass between the pressure and Coriolis terms in equation (3). A steady state is assumed. The vertical terms are small and left out following Pond and Pickard (1983) to obtain:

$$
\begin{aligned}
-v_g \cdot 2\Omega \sin\varphi &= -\frac{1}{\rho}\frac{\partial p}{\partial x} \\
u_g \cdot 2\Omega \sin\varphi &= -\frac{1}{\rho}\frac{\partial p}{\partial y} \\
0 &= -\frac{1}{\rho}\frac{\partial p}{\partial z} - g
\end{aligned}
\qquad (4)
$$

where u_g and v_g are the horizontal components of geostrophic velocity. The equation for the z direction can be written as

$$p = -\int \rho g dz \,. \qquad (5)$$

and forms the hydrostatic equation (Pond and Pickard, 1983).
The term

$$\alpha = \frac{1}{\rho}$$

that is the inverse of density is called specific volume. The difference between the in situ specific volume and the specific volume of seawater at the same pressure with S = 35 and T = 0 °C is called specific volume anomaly:

$$\delta = \alpha(S, T, p) - \alpha(35, 0, p).$$

Velocities are computed between two hydrographic stations at distance dx apart, solving the v_g from equation (4) (Pond and Pickard, 1983). The direction of the flow is from high to low pressure, and turned to the right (in the northern hemisphere) by the Coriolis force. Absolute velocities cannot be obtained, but a velocity profile relative to a constant value (traditionally a zero level, other values can be used if information is available from, for example, current meters) is obtained between the two stations perpendicular to the line connecting the stations.

3.3 Ekman velocities

The wind stress τ over the ocean makes the surface water move, causing Ekman transports in the upper layer of the ocean. The wind-forced movement diminishes with depth and veers to the right, reaching down a few tens of meters in a spiral-like manner called the Ekman spiral. Taking the horizontal equations of motion in equation (3), with the small vertical terms removed, and setting the last term to consist of surface friction gives (e.g. Pond and Pickard, 1983):

$$
\begin{aligned}
\frac{du}{dt} &= -\frac{1}{\rho}\frac{\partial p}{\partial x} + v \cdot 2\Omega \sin\varphi + \frac{1}{\rho}\frac{\partial \tau_x}{\partial z} \\
\frac{dv}{dt} &= -\frac{1}{\rho}\frac{\partial p}{\partial y} - u \cdot 2\Omega \sin\varphi + \frac{1}{\rho}\frac{\partial \tau_y}{\partial z}
\end{aligned}
\qquad (6)
$$

With the steady state assumed and the geostrophic part (equation 4) removed, the Ekman velocities are given by:

$$-v_E \cdot 2\Omega \sin\varphi = \frac{1}{\rho}\frac{\partial \tau_x}{\partial z}$$
$$u_E \cdot 2\Omega \sin\varphi = \frac{1}{\rho}\frac{\partial \tau_y}{\partial z} \quad (7)$$

where v_E and u_E are horizontal Ekman velocity components. Integrating vertically over depth gives the Ekman transport.

Over the sea bottom similar Ekman spiral currents are created by friction, but in the opposite direction than at the surface.

3.4 Volume, heat and freshwater transports

The transports of volume, heat and freshwater or salt in the ocean can be estimated if the velocities, as well as the temperature and salinity properties of the water, are known. The volume transport through a section in the ocean is computed, after velocities have first been solved, from the equation:

$$V = \sum_{i=1}^{N}\sum_{j=1}^{H(i)}\left(v_{ij}^{L}\cdot l_i^{L} + v_{ij}^{R}\cdot l_i^{R}\right)\cdot dh \quad (8)$$

where N is the number of stations in the section, dh is the pressure step the hydrographic values are averaged for, H is the number of pressure layers dh in a station half i, l is half of the width between every two neighbouring hydrographic stations, geostrophic velocity is computed between the two stations, and L and R stand for the left and right sides of a CTD station (**Fig. 6**).

In order to estimate the heat transport for the Arctic Ocean, a mass balance is required. There have been attempts (Tsubouchi et al., 2012) at closing the budget for the Arctic Ocean, but mostly the transports have been estimated using a reference temperature, resulting in a quantity sometimes referred to as relative heat transport (Losch et al., 2005)

$$Q_{rel} = \sum_{i=1}^{N}\sum_{j=1}^{H(i)} c\cdot\rho_{ij}(\theta_{ij}-\theta_{\mathrm{Re}f})\left(v_{ij}^{L}\cdot l_i^{L} + v_{ij}^{R}\cdot l_i^{R}\right)\cdot dh \quad (9)$$

where c is the specific heat capacity of water (in this work taken to be a constant 4000 $Jkg^{-1}K^{-1}$) and θ is potential temperature at 0 dbar pressure and θ_{Ref} is the reference temperature. The velocities are computed between the stations whereas the temperature and salinity values are obtained at the stations. The velocities are assumed constant between the two stations and the hydrographic properties are assumed to extend on both sides of the station to halfway between it and the neighbouring stations on either side (**Fig. 6**).

The choice of a reference salinity for freshwater estimates is less sensitive and freshwater transports can be computed from

$$Fw_{rel} = \sum_{i=1}^{N} \sum_{j=1}^{H(i)} \rho_{ij} (S_{\mathrm{Re}\,f} - S_{ij}) / S_{\mathrm{Re}\,f} \left(v_{ij}^{L} \cdot l_i^{L} + v_{ij}^{R} \cdot l_i^{R} \right) \cdot dh \qquad (10)$$

where S_{ij} is salinity and S_{Ref} is the reference salinity.

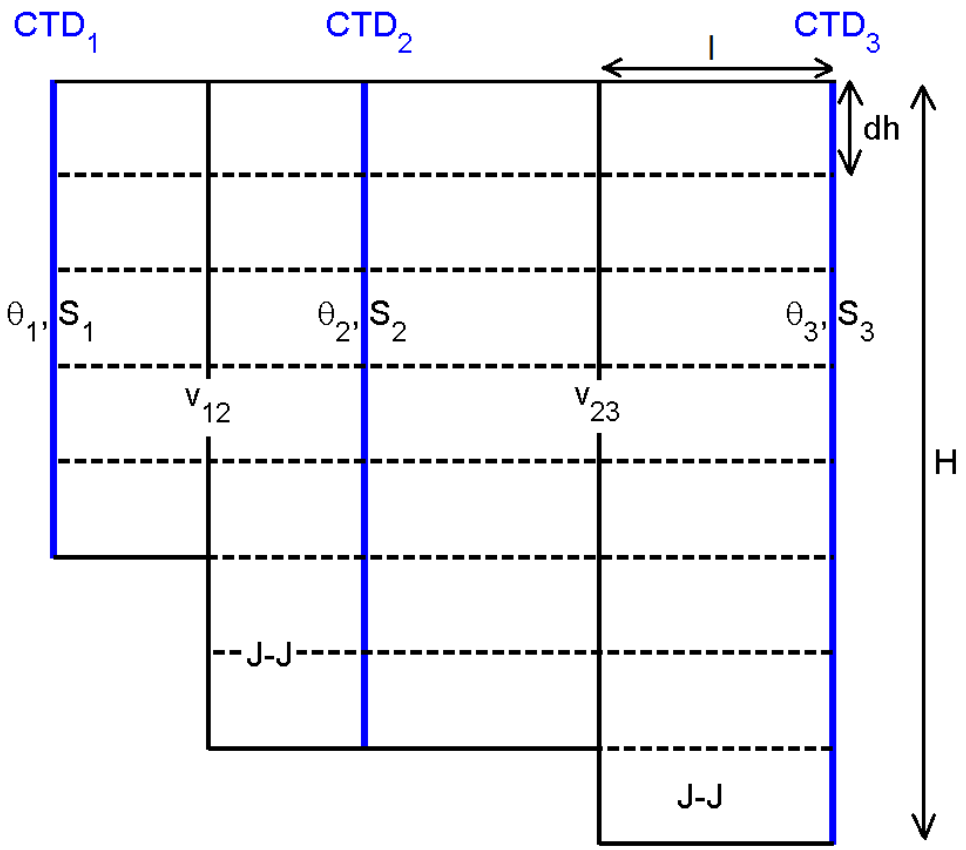

Figure 6: Schematic of CTD stations, θ and S properties, geostrophic velocities and Jacobsen and Jensen (J-J) extension. H is the number of thickness layers dh and l is half of the width between two neighbouring CTD stations.

3.5 Water mass properties and changes

Waters of different origin can be distinguished based on their temperature and salinity properties (Nansen, 1902; Helland-Hansen, 1918; Sverdrup et al., 1942; Mamayev, 1975; Emery and Meincke, 1986). Other additional parameters, e.g. oxygen, phosphate, nitrate, silicate (Jones and Anderson, 2008; Tanhua et al., 2009) or transient tracers such as chlorofluorocarbons (CFCs) or sulphur hexafluoride (SF_6) of anthropogenic origin can also be used (Bönisch and Schlosser,1995; Watson et al., 1999).

The properties of the water masses can be used to trace them to their areas of formation and thus information about the ocean circulation can be obtained. The observed changes in the water masses are a combination of changes undergone in the area of formation of the water mass, i.e. warming due to atmospheric warming, and of changes undergone by the water mass along the way. Distinguishing between the two can be difficult. Using tracers can be useful for following circulation patterns and for distinguishing water masses of different origin (e.g. Karcher et al., 2012).

Water masses represented in a θS diagram inside a triangle can be separated into fractions between 0 and 1 of source water whose temperature and salinity properties are located at the vertices of the triangle (Mamayev, 1975) (**Fig. 7**). Heat conduction and diffusion, and advection are not included in the triangle computations. The fractions *f* are solved from equations:

$$\begin{aligned} f_1 \cdot S_1 + f_2 \cdot S_2 + f_3 \cdot S_3 &= S_i \\ f_1 \cdot \theta_1 + f_2 \cdot \theta_2 + f_3 \cdot \theta_3 &= \theta_i \\ f_1 + f_2 + f_3 &= 1 \end{aligned} \qquad (11)$$

The water masses in the Fram Strait and in the Nordic seas are shortly described in the methods section 5.7.

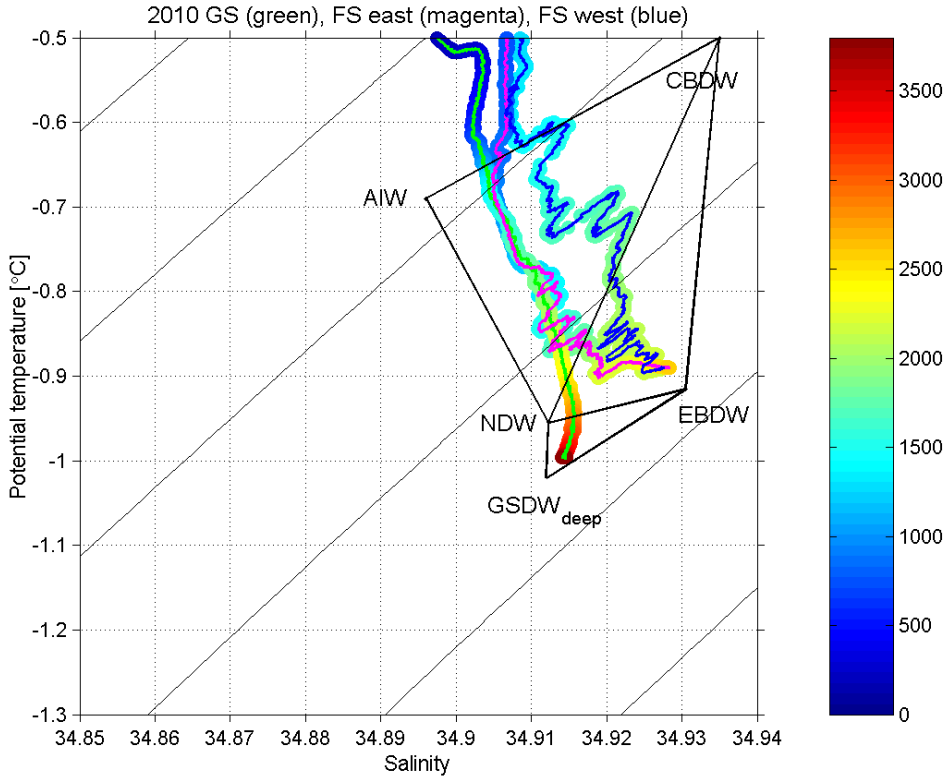

Figure 7: An example of water mass triangles. All the (S_i,θ_i) values inside a triangle can be expressed with fractions of the potential temperature and salinity values at the vertices (equation 11). From paper V, Figure 4.

4 Observations

4.1 Hydrographic data

The core of this work is based on hydrographic observations made onboard research vessels with profiling CTD (Conductivity, Temperature, Depth / pressure) instruments. The CTD system typically involves an underwater unit with sensors, a frame that the underwater unit and water sampler are attached to, a winch and a cable used for lowering the CTD to the sea, a deck unit, and related software. Salinity, the amount of dissolved salts in the water, is computed from conductivity, temperature and pressure. The data are processed using coefficients from factory / laboratory calibration and salinities obtained from the water samples, and analysed with a salinometer. Missing or erroneous near surface values are extrapolated to the surface using constant values. The largest error spikes in salinity are removed.

Observations from the Fram Strait and its vicinity as well as from the Greenland Sea are used to study water mass properties and to estimate transports of volume, heat and freshwater. The transports are computed through sections consisting of CTD stations (**Table 2**). This allows for forming rather long time series with better horizontal and vertical resolution than from the current meter moorings present at the strait. Eddies can still pass the section without being fully recognized if they are only observed in one station due to sparse station spacing. Helland-Hansen (1918) pointed out already in 1904 how the removal of a single station from between two others may entirely alter the appearance of the section. The temporal resolution from hydrographic sections is worse (usually once a year) and biased due to most observations being from summertime (Schauer and Beszczynska-Möller, 2009, Fig. 5; de Steur et al., 2014).

In paper I 16 hydrographic sections from 1980-2005 are obtained in the Fram Strait along about 79 °N, reaching from the Greenland shelf to the slope west of Spitsbergen. In papers II and IV two hydrographic sections at latitudes between 81 °18 'N and 82 °20 'N from IB Oden are combined to reach from north of Svalbard to the Greenland shelf. In papers III (preliminary results) and IV, additional hydrographic sections north of the 79 °N section in the Fram Strait are available for the years 1984, 1997 and 2004, from which the highest latitude in 2004 at about 83 °N, can be combined with the 79 °N section. In paper IV a meridional section at 0 °E has been taken for the years 1997, 2001 and 2003. In paper V two hydrographic sections, one across the Fram Strait at about 79 °N and the other at 75 °N in the Greenland Sea are combined for years 1999-2002, 2004, 2005, 2008 and 2010 (**Figs. 8, 9**).

Auxiliary CTD data are used for studying the water mass properties from the late 1970s to 2013 varyingly from the Greenland Sea, the Fram Strait and the Norwegian Sea, and from the Arctic Ocean in paper V. Data from the Arctic Ocean taken by MV XueLong in 2008 are studied in paper III. Most data available are from summertime (June to September).

Table2. Cruises and years for full sections discussed in the included papers.

Ship	Year	Number of FS stations	Number of GS stations	Number of northern stations	Paper
IB Ymer	1980	20	-	-	I, III
RV Lance	1983	23	-	-	I, III
RV Lance	1984	20	-	27	I, III, IV
RV Polarstern	1988	18	-	-	I, III
RV Polarstern	1993	17	-	-	I, III
RV Lance	1997	18	-	-	I, III, IV
RV Polarstern	1997	-		24	IV
RV Polarstern	1998	34	-	-	I, III
RV Polarstern	1999	34-38	60	-	I, III, V
RV Polarstern	2000	36	57	-	I, III, V
RV Lance	2000	31-35	-	-	I, III, V
RV Polarstern	2001	39	-	-	I, III, V
RV Polarstern	2002	72-73	-	-	I, III, V
IB Oden	2002	-	-	21	II, III
RV Polarstern	2003	50	-	-	I, III
RV Lance	2003	32	-	-	I, III
RV Polarstern	2004	49-51	55	35	I, III, IV, V
RV Polarstern	2005	74-76	56	-	I, III, V
RV Polarstern	2008	58	52	-	V
RV Polarstern	2010	79	62	-	V

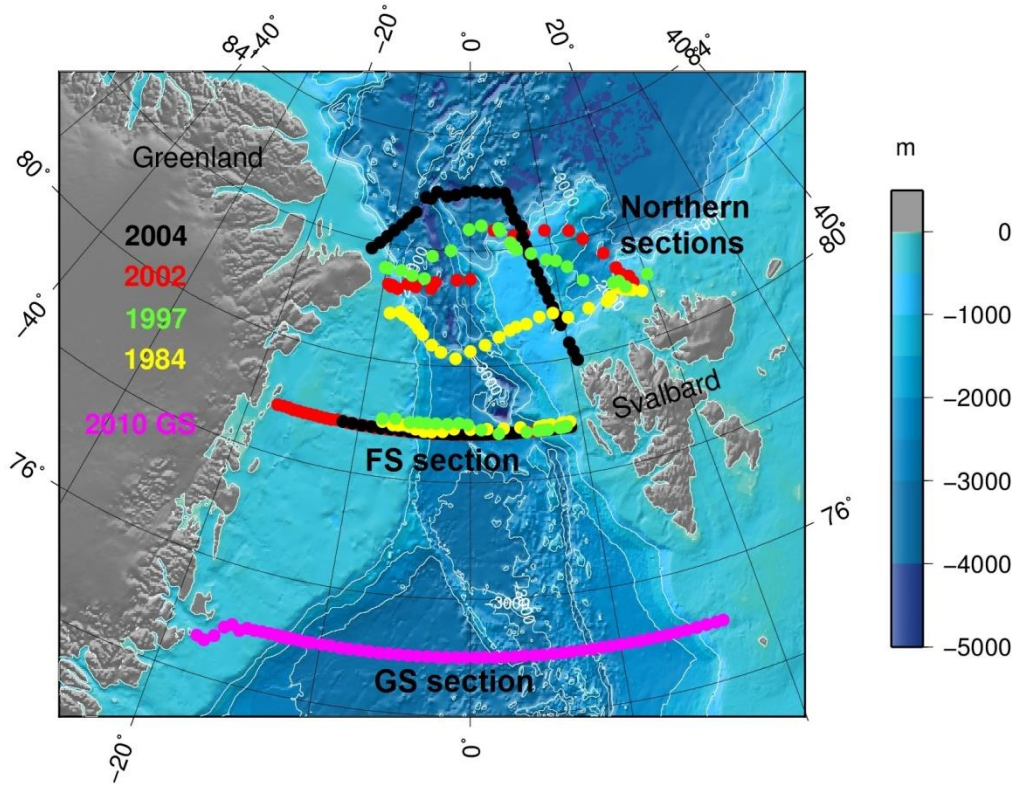

Figure 8: Section / station locations. The standard sections in the Fram Strait at about 79 °N and in the Greenland Sea at 75 °N vary in length annually, the maximum coverages are shown. All northern sections and their years are shown.

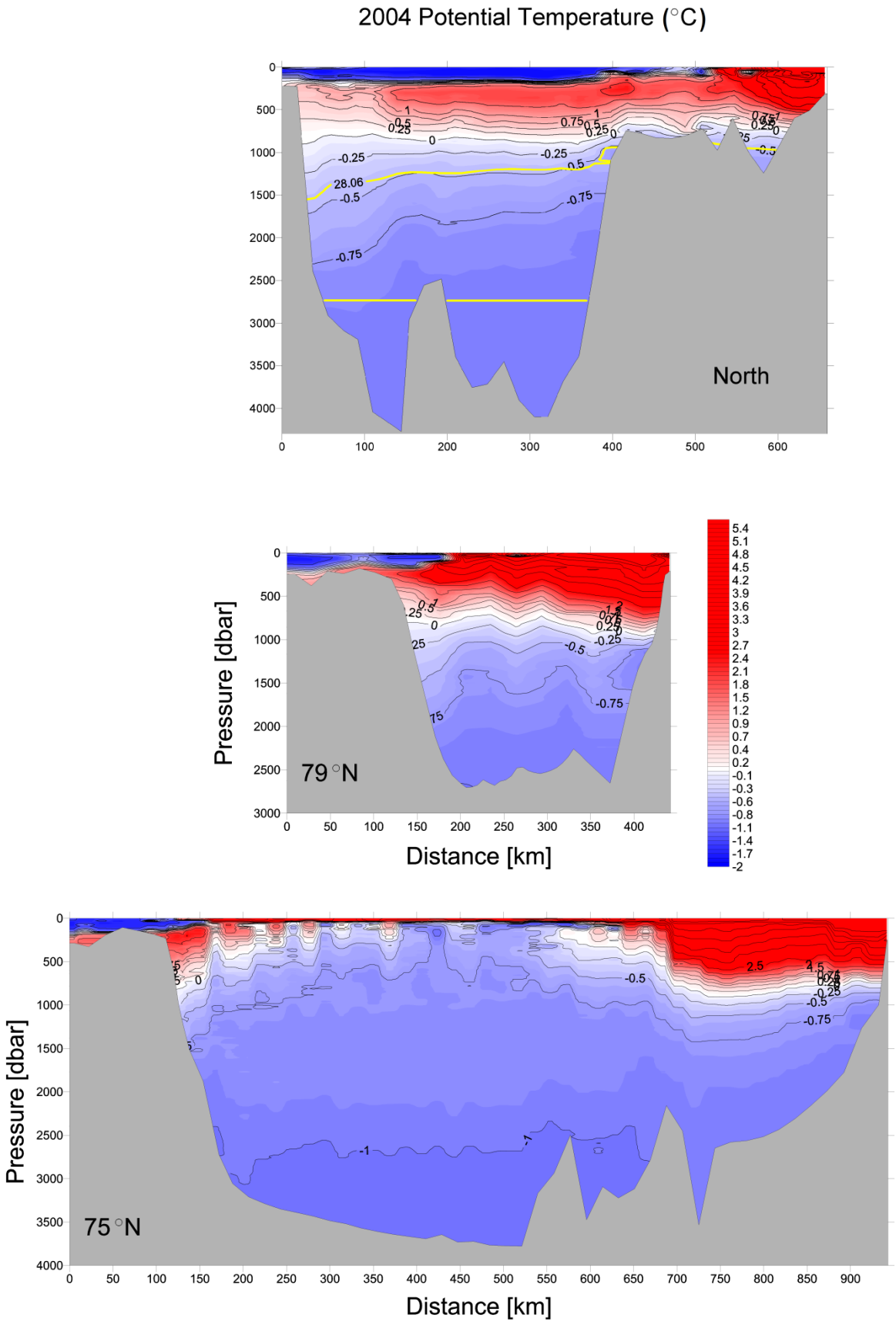

Figure 9a: Potential temperature sections for 2004. Northern, Fram Strait and Greenland Sea sections. From papers IV and V.

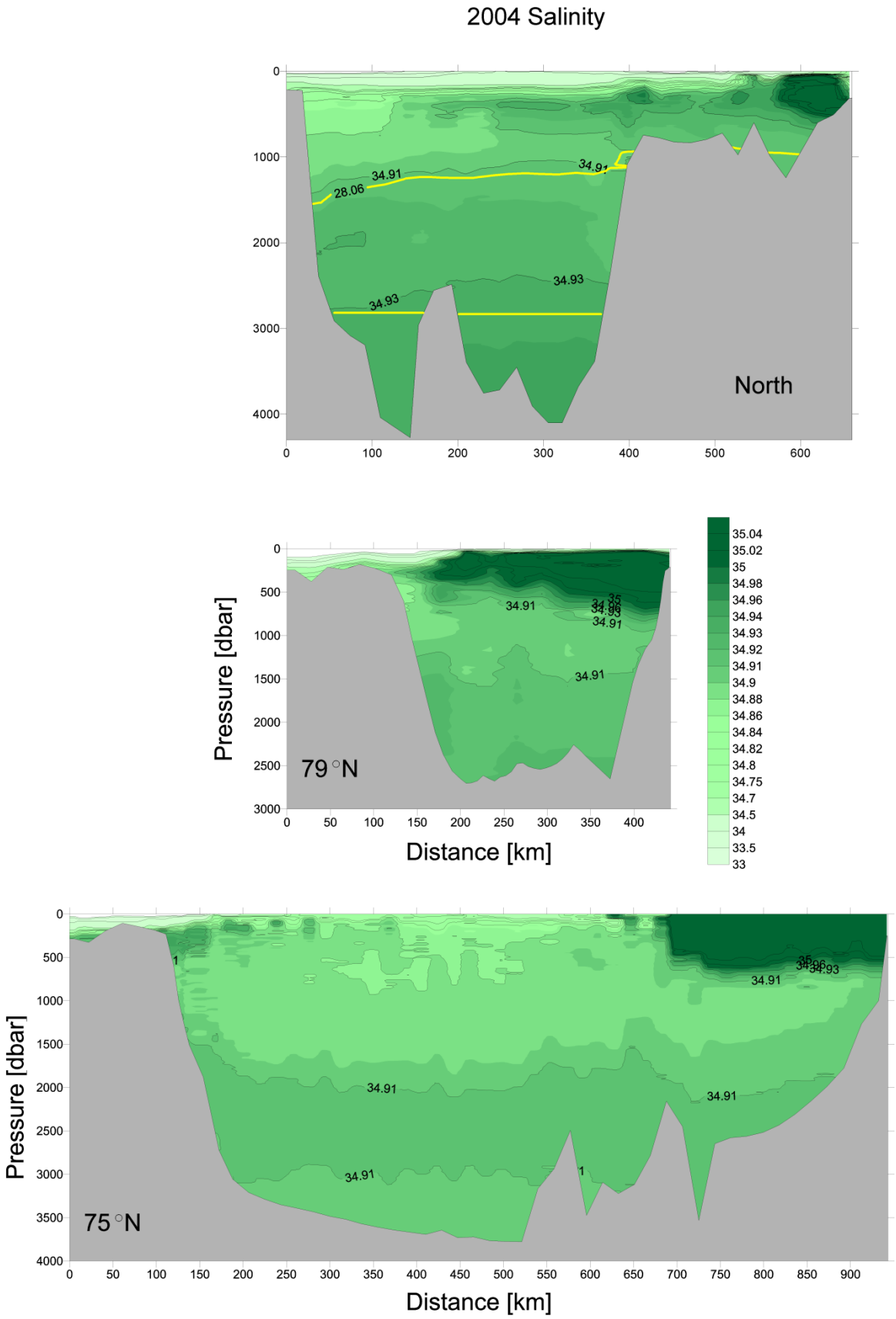

Figure 9b: Salinity sections for 2004. Northern, Fram Strait and Greenland Sea sections. From papers IV and V.

4.2 ADCP data

The currents in the ocean can be measured directly using an Acoustic Doppler Current Profiler (ADCP). The CTD frame on IB Oden in 2002 was equipped with dual (upward and downward looking) 300-kHZz RDI Workhorse ADCPs. On the two northern sections in papers II and IV the currents were measured using this lowered ADCP (lADCP). Vessel-mounted ADCP data from a narrow band 150 kHz ADCP from RD instruments are available from RV Polarstern in 2004 reaching from 25 m to a maximum depth of 425 m. Both lADCP and vessel-mounted ADCP data were processed and subsequently detided by subtracting tidal velocities obtained from a high-resolution barotropic inverse tidal model (Padman and Erofeeva, 2004).

4.3 Argo data

Argo is a pilot program of the Global Ocean Observing System. Close to 4000 Argo floats are currently drifting with the ocean currents worldwide. The Argo floats are set to float at a fixed pressure and are equipped with sensors (to obtain at least temperature, salinity and pressure) to measure profiles every 10 days between a maximum depth of 2000 dbar and the surface. Most of the floats used in this study had a parking depth of 1000 dbar where they float with the currents. Argo data are collected and made freely available by the international Argo program (http://www.argo.net). Argo data are available online for the Greenland Sea from 2001 onward and for the Fram Strait from 2006 onward.

4.4 Tracer data

Transient tracer sulphur hexafluoride (SF_6) was released in a mixing experiment in the Greenland Sea in 1996 in the intermediate water layer, and spread from the source of release with circulation (Watson et al., 1999). It also has an atmospheric, anthropogenic origin, mainly industrial. In 2002 SF_6 was still present in and near the Greenland Sea in concentrations exceeding the anthropogenic background levels. It was sampled on the Oden cruise with water sample bottles attached to the CTD frame, its concentration was determined with purge-and-trap pre-treatment and electron-capture-detection, and the atmospheric concentration was removed to produce an excess SF_6 concentration. Excess SF_6 concentrations between positive values are linearly interpolated to match the CTD pressure interval of 1 dbar and linearly extrapolated to go to zero from the deepest and shallowest positive values.

5 Data analysis methods

5.1 Geostrophic computations

Geostrophic velocities are computed to obtain volume transports through hydrographic sections. The geostrophic method assumes a balance with the pressure and Coriolis terms in equation (3), and ignores the barotropic, pressure independent component. A velocity shear is obtained, but no absolute velocities. Traditionally a level of no motion is chosen. Here we start by setting velocity to zero close to the bottom in all cases except for paper II, in which a zero value is applied to the surface velocity at the eastern section.

5.2 Jacobsen and Jensen extension near bottom

The geostrophic velocities are computed between two neighbouring stations with the depths of the station casts often unequal. Some deep transports are therefore missed at the deeper station cast of the station pair. The method of Jacobsen and Jensen (1926) is used to estimate the velocities at the deeper station at all levels j located below the deepest common level of the station pair (where i represent the shallower station and i+1 the deeper) by extrapolating the difference in the specific volume anomalies δ between the two stations at the level of the bottommost measurement of the shallow station to the bottom of the deeper station. The velocity is obtained by dividing the anomaly difference $\Delta\delta_i$ by the distance L_i between the stations and by the Coriolis term f ($f = 2\Omega sin\varphi$), and multiplying by a depth-dependent sum. For layers j of thickness dh below the shallow station (**Fig. 6**), we get

$$v_{i+1,j} = \frac{\Delta\delta_i}{L_i f} \sum_{k=1}^{j} (\Delta H_i - k \cdot dh) / \Delta H_i \qquad (12)$$

where $j = 1, \ldots, \Delta H_i/dh$ and ΔH_i is the difference between the bottom depth of the deep station and the bottom depth of the shallow station.

Direct current observations in the Fram Strait have shown a northward flow in the WSC at the eastern slope and a southward flow in the EGC at the western slope (Aagaard et al., 1973; Fahrbach et al., 2001; Schauer et al., 2004). The velocity on the slopes is therefore set to zero at either the bottom of the shallow station cast or at the bottom of the deep station cast in order to have the flow in that part that is deeper than the maximum depth of the shallow station move northward in the east and southward in the west, i.e. in the direction indicated by the direct current observations (see paper IV, Fig. 6).

5.3 Constraints and minimization

The transports estimated from geostrophy without knowledge of the actual velocities at any depth are improved by setting constraints on the transports and using a variational method (Wunsch, 1978; Houssais et al., 1995). In paper I with only one

section available the deep transports are assumed constant for years 1980 to 2005 in the Fram Strait and a net volume transport of 0.4 Sv southward of deep water with $\sigma_\theta \geq$ 28.06 kg/m^3 is required, consisting of volume transports of 0.2 Sv northward and 0.6 Sv southward with mean salinities 34.91 and 34.9325 respectively, providing an additional constraint for net salt transport. The constraints are mainly applied to ensure that the more saline Arctic Ocean waters to the west would flow southward and the less saline Nordic Seas waters in the east northward when the kinetic energy in the next step is minimized and the flow field solved for the two constraints below the 28.06 kg/m^3 isopycnal.

In paper II two zonal sections north of the Fram Strait separated by a gap are combined for 2002. The velocities are set to zero at the bottom of the western section and at the surface of the eastern section. No constraints for the deep part can be set due to the gap. An additional constraint is required for the part of the eastern section crossing the Sofia Deep allowing no net transport across the Sofia Deep below 700 dbar (**Figs. 1, 8**).

In papers IV and V two zonal sections are available and conservation constraints are formulated on quasi-closed boxes in a way similar to Houssais et al. (1995)

$$\iint_{\gamma} v^b(x) R(x,z)\,dxdz + \iint_{\gamma} v^{bc}(x,z) R(x,z)\,dxdz = C \qquad (13)$$

where $v^b(x)$ is the depth-independent barotropic velocity, $v^{bc}(x,z)$ is the baroclinic velocity from the geostrophic computations, R is either S for salt transport, θ for heat transport or 1 for volume transport and γ stands for the area of the CTD sections on which the constraint is applied. In papers IV and V the boxes are assumed to have no sources or sinks and the constraints C become equal to zero.

The constraints are as follows in paper IV: 1) Salt is conserved in the whole box, which allows for freshwater input or output in the area e.g. due to ice melt or formation, 2) volume, 3) salt and 4) heat are conserved below isopycnal 28.06, i.e. below the influence of atmosphere and local convection as well as separated from the Sofia Deep east of the Yermak Plateau, and above the Fram Strait sill depth, 5) volume is conserved in the northern section below the Fram Strait sill depth, 6) volume is conserved in the Sofia Deep below the depth at which waters are not expected to cross between Sofia Deep and the Fram Strait proper (See **Fig. 8**, years 1984-2004 for the section locations).

In paper IV two additional boxes are formed to estimate the recirculation (See paper IV, Fig. 4), where transports are estimated through a meridional section. The constraints 2) - 4) are applied.

The constraints in paper V are 1) salt is conserved in the whole box, 2) volume and 3) salt are conserved below the approximate maximum Greenland Sea convection depth during the observation period, and above the Fram Strait sill depth, 4) volume is conserved in the Greenland Sea below the Fram Strait sill depth.

The barotropic velocity components v^b are computed by minimizing the kinetic energy of the barotropic part using the method of Lagrangian multipliers (Lanczos, 1970; Wunsch, 1978; Stommel and Veronis, 1981). The barotropic reference velocities are determined by solving the Moore-Penrose inverse.

5.4 Transports from ADCP velocities

Current velocities can be directly measured with ADCP instruments. In the Fram Strait an array of moored current meters has been maintained regularly since 1997 by the Alfred Wegener Institute from Germany and the Norwegian Polar Institute, providing information on the general circulation patterns in the strait and the variability and seasonal signals of the currents (Fahrbach et al., 2001; Schauer et al., 2004; Schauer and Beszczynska-Möller, 2009; de Steur et al., 2014; von Appen et al., 2015). These data, although providing good temporal coverage, are spatially sparse (e.g. Schauer and Beszczynska-Möller, 2009, Fig 2). In this study ADCP data measured from onboard two research vessels (IB Oden in 2002 and RV Polarstern in 2004) are used.

LADCP velocities have the same horizontal coverage as the CTD measurements and are averaged to 10 m bins from close to the surface to the depth of the station cast (paper II). LADCP data are available from the two sections north of the Fram Strait in 2002 and are used to compute volume transports. A velocity component perpendicular to a line connecting the CTD station locations is chosen in order to compare the results with those from geostrophy.

Vessel-mounted ADCP provides current information for the uppermost few hundred meters along the cruise-track. These data are used in paper IV to estimate transports for the two uppermost water masses: surface water (averaged over 35-55 m) and AW (averaged over 155-255) and to compare the results to those from geostrophy.

5.5 Drift derived from Argo floats

Profiling Argo floats are measuring the hydrography and drift in the oceans year-round, in the Greenland Sea since 2001. In paper V two sections, one from the Fram Strait at 79 °N and the other crossing the Greenland Sea at 75 °N, are combined. The drift estimated from the Argo floats is used to modify the geostrophic velocities. The flow in the Greenland Sea is cyclonic along the rims of the deep basin (e.g. Voet et al., 2010). The drift is estimated from Argo floats with parking depths mainly at 1000 dbar and some at 1500 dbar, considered to be representative of the drift at 1000 dbar by Voet et al. (2010). Argo velocities are estimated from two consequent surface observations: the last location before the dive and the first location after the dive. The computed velocity is assigned to a midpoint between the two locations. The Argo-based velocities are averaged over 1 degree squares at 75 °N latitude. The cyclonic flow is visible as large southward velocities in the west and northward velocities in the east. A linear fit is found for the Argo float derived velocities at 75 °N and used to modify the geostrophic velocities before applying the 4 constraints in paper V.

5.6 Heat and freshwater transports

The heat and freshwater transports through the Fram Strait have an important impact on the Arctic climate. With the observations covering the Fram Strait, but not the other gateways to the Arctic Ocean, namely the Barents Sea, Bering Strait, and CAA, the transports to and from the Arctic Ocean cannot be balanced. The transports of relative heat and freshwater are nevertheless computed relative to a reference temperature and salinity, but the results are rather arbitrary (Schauer and Beszczynska-Möller, 2009; Tsubouchi et al., 2012).

In paper I the volume transports are computed through a section located in the Fram Strait. The relative heat transport is computed relative to the mean temperature of the southward flow and the freshwater transport relative to the mean salinity of the northward flow so that the mean southward flow carries no heat and the mean northward flow carries no freshwater. The largest possible transports of heat and freshwater with the estimated velocities through the strait are obtained.

Heat loss and freshwater gain are estimated inside a box closed by the 79 °N section in the Fram Strait and a northern section (paper IV) or a Greenland Sea section at 75 °N (paper V) (**Fig. 8**).

5.7 Water mass definitions

Waters in the ocean of different origin are traditionally defined using temperature-salinity curves (e.g. Helland-Hansen, 1918; Mamayev, 1975). Chemical and biological observations can also be used for further separation of the water mass origins (e.g. Jones and Anderson, 2008). In this work, six water mass classes are defined (**Table 3**, from e.g. paper V, Table A2), separated mainly by isopycnals based on and simplifying the classification of Rudels et al. (2005): surface water, AW, dense Atlantic water (dAW), intermediate water and deep water layers I (less dense) and II (more dense). In the figures and in their interpretation some water masses are divided further, as in Rudels et al. (2005): surface water is subdivided into warm and cold surface waters along the 0 °C isotherm; AW is divided by the 2 °C isotherm into colder Arctic Atlantic water (AAW) that has circulated in the Arctic Mediterranean, and into warmer Atlantic water from the south; deep waters are separated according to a salinity of 34.915 into the less dense Nordic Seas Deep Water (NDW) and Arctic Ocean derived deep waters: Canadian Basin Deep Water (CBDW) in the Deep Water I densities, and Eurasian Basin Deep water (EBDW) in the Deep Water II densities (e.g paper I, Figure 13.5).

The surface water in the Fram Strait and Nordic Seas contains sea ice melt water, river runoff and precipitation, AW that has been diluted with them, and occasionally water of Pacific origin (e.g. Falck et al., 2005; Rabe et al., 2013; Rudels et al., 2013). In this work, any water mass with sufficiently low density is defined as surface water.

In paper IV the amount of AW recirculating in the Fram Strait is estimated from the density-based water mass classification for AW, and from the volume transports.

In paper II the intermediate layer is divided into AIW and uPDW based on the excess SF_6 contained in the 2002 data that is present in the AIW originating from the Nordic Seas. The AIW forms a salinity minimum, and during the earlier years also a temperature minimum near its origins, but separating the two water masses based on the temperature and salinity curves in a θS diagram is only possible for the most typical profiles close to their origins.

In paper V a triangle method (Mamayev, 1975) is used to describe the properties of the deep water masses in order to distinguish between waters of Arctic Ocean and Nordic Seas origins, as the Greenland Sea deep water has gradually become warmer and more saline making it impossible to identify the deep waters in the Fram Strait based on their salinities only. Three triangles are formed with the following vertices: 1) AIW - CBDW - NDW, 2) EBDW - NDW - CBDW, and 3) EBDW - GSDW - NDW, where GSDW is the Greenland Sea Deep water (**Fig. 7**). Water mass values inside the triangles can be described as mixtures of the water mass properties found at the vertices, whose proportions can be solved from equations (11).

Table 3: Water mass definitions from Rudels et al. (2005) and paper I.

Water masses	**Density Range**	**Nordic Seas water masses**	**Arctic Ocean water masses**
Surface water	$\sigma_\theta<27.70$	warm Surface Water (wSW)	Polar Surface Water (PSW)
Atlantic water	$27.70\leq\sigma_\theta<27.97$	Atlantic Water (AW)	Arctic Atlantic Water (AAW)
dense Atlantic water	$\sigma_\theta\geq27.97$ $\sigma_{0.5}<30.444$, $\theta>0$	dense Atlantic Water (dAW) S & θ decreasing with depth	dense Arctic Atlantic Water (dAAW) S increasing, θ decreasing with depth.
Intermediate water	$\sigma_\theta\geq27.97$, $\sigma_{0.5}<30.444$, $\theta\leq0$	Arctic Intermediate Water (AIW) upper S & θ decreasing with depth, lower S & θ increasing with depth	upper Polar Deep Water (uPDW) S increasing, θ decreasing with depth.
Deep Water I	$\sigma_{0.5}\geq30.444$, $\sigma_{1.5}<35.142$	Nordic Seas Deep Water I (NDWI), S<34.915	Canadian Basin Deep Water (CBDW)
Deep Water II	$\sigma_{1.5}\geq35.142$	Nordic Seas Deep Water II (NDWII), S<34.915	Eurasian Basin Deep Water (EBDW)

6 Results

6.1 Volume transports

Oceanic transports between the Arctic Ocean and the Nordic Seas through the Fram Strait are in this work estimated from hydrographic sections taken between 1980 and 2010 (**Table 2, Figs. 8, 9**). In paper I the net volume transport obtained from geostrophy with constraints applied on deep waters and averaged over 1980 to 2005 (summertime snapshots) is 2.5 ± 1.3 Sv southward, with an additional 0.3 Sv over the Greenland continental shelf. The obtained mean net transports are balanced with transport estimates at the other passages to the Arctic Ocean: Bering Strait, CAA, and the Barents Sea Opening, as well as with river runoff and precipitation - evaporation, and the volume transport is reduced to 1.7 Sv southward. The northward and southward flows range from 5 Sv to almost 15 Sv with an average inflow to the Arctic Ocean of about 6 Sv and an outflow of about 9 Sv (**Fig. 10**). In paper I it is estimated that more than 60% of the inflow to the Arctic Ocean and 80-90% of the outflow pass through the Fram Strait.

The volume transports are also estimated in papers II, IV and V, and preliminarily in paper III similarly to paper IV. In paper II the section is located north of the standard 79 °N section and has a gap in the middle. The net volume transport to the east of the gap is 3.6 Sv northward and to the west of it 5.1 Sv southward. At the gap the transport is roughly estimated at 0.5 Sv northward resulting in a net volume transport across the whole section of 1.0 Sv. The transports are also estimated for the 2002 northern section using lADCP data, resulting in about three times larger northward and southward volume transports with a net transport that is close to zero. Errors may be due to the gap in the section, to two of the deep stations not reaching deeper than 1200 dbar, to the step-like bathymetry used to calculate the transports at the slopes or to poorly-resolved de-tiding near the Yermak Plateau.

In papers IV and V quasi-closed boxes are formed and the transports are balanced by applying constraints. In paper IV the transports are estimated through sections in the Fram Strait and north of it. The net volume transport obtained for four years between 1984 and 2004 vary between 2 and 4 Sv averaging at 3.1 Sv, with the northward and southward transports about 10 Sv or less (**Fig. 10**).

In paper V the transports are estimated through sections in the Fram Strait and across the Greenland Sea along 75 °N. The net volume transports are first estimated at 1.9 ± 1.0 Sv southward, a rather similar result to the estimates in the previous papers. When velocities estimated from the Argo floats are used to modify the velocities at 1000 dbar depth in the Greenland Sea section, the transports are reduced to 0.8 ± 1.5 Sv southward. The northward volume transports are in the Greenland Sea section 16 ± 2 Sv and southward 17 ± 2 Sv. In the Fram Strait section the volume transports are 10 ± 3 Sv northward and 11 ± 3 Sv southward (**Fig. 10**). Woodgate et al. (1999) estimated the southward transport within the EGC at 21 ± 3 Sv through the Greenland Sea section, with a minimum of 11 Sv in summer and maximum of 37 Sv in winter, based on current meter moorings in 1994-1995. The results obtained in this work are reasonable, although geostrophy is expected to underestimate the northward and southward transports since the barotropic currents are not appropriately resolved.

The individual northward and southward volume transports increase toward the end of the 1980-2005 period, which is likely due to the denser station spacing in the

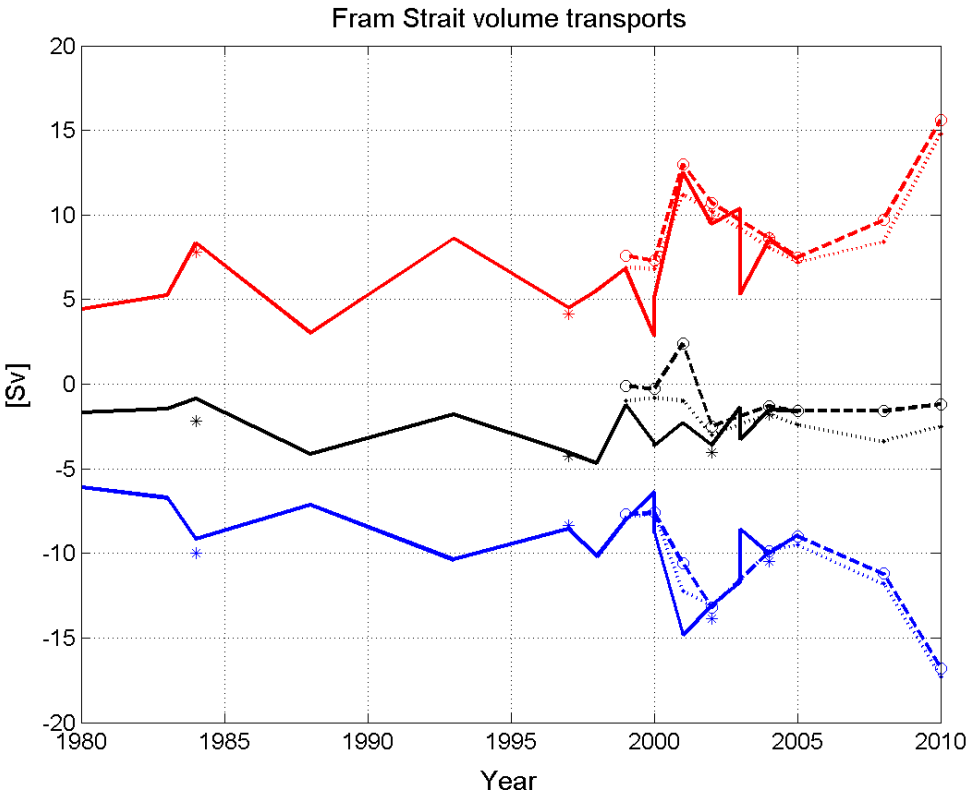

Figure 10. Volume transports through the Fram Strait. Red northward, blue southward, and black net. Solid line 1980-2005 time series with deep constraints, stars: 1984-2004 from quasi-closed boxes, dashed line: 1999-2010 time series from quasi-closed boxes with Argo adjustment, and dotted line: 1999-2010 from quasi-closed boxes without Argo adjustment

later years allowing for more eddies to be at least partially captured. The net volume transports between 1980 and 2010 are variable but do not show a trend (**Fig. 10**). The choice of constraints affects the results (see paper IV, Table A1) as does the chosen level of no motion, or in the case of a reference velocity e.g. from the Argo floats (paper V), level of "known motion".

The box method in paper V gives a possibility to estimate the deep transport that was assumed to be a constant 0.4 Sv southward below the 28.06 isopycnal in paper I for the time period 1980-2005. The deep transports in the Fram Strait estimated from the Fram Strait - Greenland Sea double sections, with Argo adjustment and 4 constraints applied, and with northward transport positive and southward transport negative, are shown in **Table 4a**:

Year	V northward [Sv]	V southward [Sv]	V net [Sv]
1999	0.89	-0.99	-0.11
2000	0.86	-0.76	0.09
2001	1.70	-0.69	1.01
2002	1.34	-1.99	-0.65
2004	0.75	-1.29	-0.53
2005	0.94	-1.34	-0.41
2008	1.48	-1.14	0.34
2010	2.09	-2.13	-0.05

giving a mean deep volume transport -0.10 ± 0.61 Sv for the time period 1999-2005, overlapping with the period in paper I. Excluding 2001, which has a northward net volume of about 2 Sv, gives -0.32 ± 0.31 Sv. This is close to the -0.4 Sv used in paper I.

Applying the four constraints but without the Argo adjustment gives **Table 4b**:

Year	V northward [Sv]	V southward [Sv]	V net [Sv]
1999	0.71	-0.92	0.21
2000	0.76	-0.77	-0.01
2001	1.17	-1.06	0.11
2002	1.31	-1.88	-0.57
2004	0.79	-1.15	-0.36
2005	0.98	-1.30	-0.31
2008	1.13	-1.26	-0.13
2010	2.04	-2.15	-0.10

with a mean deep volume transport -0.15 ± 0.30 Sv for the time period 1999-2005.

The zonal sections in the Fram Strait and in the Greenland Sea are divided into 4-5 sub-sections: The Svalbard slope; the deep basin divided in two by the Greenwich meridian; and the Greenland continental shelf slope. The Greenland shelf, or its eastern part, is included as a 5th section part when data are available. The volume transports are up to 1 Sv southward over the Greenland continental shelf, but average to about 0.3-0.5 Sv southward in paper I and 0.4 ± 0.4 Sv southward in paper V. The most consistent southward flow is found over the western slope and northward in the WSC over the eastern, Svalbard slope.

6.2 Water mass properties

The upper layer water mass properties vary quite significantly depending on which part of the Fram Strait or the 75 °N section they are located in, with the coldest, least saline, and least dense surface water located in the Greenland continental shelf and slope. In the eastern parts of the sections in particular, AW can be found in the surface layer. The surface waters in the Fram Strait section are in general colder, less saline, and especially in the western slope less dense than at the 75 °N section. The surface waters in the section north of the Fram Strait are colder than at the Fram Strait section and tend to become less saline as they flow southward to the Fram Strait, reflecting ice melt in between sections.

The Atlantic waters are most saline and warmest in the eastern parts of the Fram Strait and the 75 °N section where the net volume flow of AW is northward. The warmest and most saline AW is found at the 75 °N section and coldest and least saline at the sections north of the Fram Strait. Besides the recirculation in the Fram Strait, part of the southward-flowing AW has circulated in the Arctic Ocean and become cooled and due to mixing less saline. As this southward flowing AAW (Rudels et al., 2005) mixes with the surrounding waters it becomes warmer and more saline in the more southern sections (**Fig. 9**).

Warm anomalies of AW were first reported to occur in the Fram Strait and continue into the Arctic Ocean by Quadfasel et al. (1991). A more recent warm pulse took place in 2005-2006 (e.g. Walczowski et al., 2012). During the 1999-2010 time

series AW has become about 0.4 °C warmer and 0.005 more saline largely due to the mid-2000s warm anomaly. In the earlier 1980-2005 time series, the warm and saline AW can also be found in the Fram Strait in 1983 and 1984. The difference between the northward- and southward-flowing AW in the Fram Strait varies between 0.0 and 1.0 °C, being about 0.6-0.7 °C during 1983-1984, otherwise smaller in the 1980s, and with the largest differences occurring in the late 1990s. During the 1999-2010 the difference between the northward- and southward-flowing AW in the Fram Strait has diminished from 0.4 to 0.1 °C. A likely cause for the reduction in the temperature difference in the Fram Strait is the warmer westward recirculation in the Fram Strait in the 2000s reported by e.g. Beszczynska-Möller et al. (2012) and de Steur et al. (2014). In the 75 °N section the temperature difference between northward and southward AW remains at about 0.5 °C during 1999-2010. From 1984, 1997, 2002 and 2004 northern sections the AW is found to have a difference of 0.1-0.4 °C between the northward and southward transports. The difference between the northward-flowing AW in the Fram Strait section and the northern section varies between 0.6-0.9 °C. In the southward flow the difference shows greater variation, partly due to the different locations of the northern section. The northern-most section is from 2004, the difference between the northern section and the Fram Strait section then is 1.5 °C, perhaps reflecting the warm recirculation in the Fram Strait, but also the presence of more, cooler AAW returning southward. The dAW properties show similar variability to that of AW.

The intermediate waters are separated into AIW and uPDW in paper II based on excess SF_6 concentrations. The salinity minimum of AIW is created in the Nordic Seas by the convection of low-salinity water to the deeper layers. It can be used to distinguish AIW from uPDW that has formed within the Arctic Ocean, especially at stations close to its formation. Further away from the source the signature becomes weaker as the water masses mix with surrounding waters. AIW in the Greenland Sea has become warmer and more saline in the 2000s which is reflected in the averaged intermediate water properties.

The intermediate and deep waters have become warmer and more saline during the observation period, especially in the Greenland Sea. In the Fram Strait the trend in salinity is not clear and there are more fluctuations, especially in the intermediate water properties, similar to that found in AW.

The deep waters have in this work been separated in two density classes, but also based on their Arctic Ocean or Greenland Sea origins by a constant salinity 34.915 (**Table 3**; Rudels et al., 2005; paper I). Since the salinity of the GSDW has increased due to a weakened convection and interaction with the Arctic Ocean deep waters (Budéus et al., 1998), this separation is no longer valid, and deep waters have therefore also been separated using water mass triangles in paper V (**Fig. 7**). While the deep waters have in general also become warmer during the three decades studied in this work, the changes in the Arctic Ocean are much smaller than in the Greenland Sea. The intermediate and deep waters in the in the sections north of the Fram Strait are warmer and more saline than the corresponding water masses in the Fram Strait section, showing a greater influence from the Arctic Ocean deep waters. The deep waters continue to be warmer and more saline at the Fram Strait than at the Greenland Sea section. The GSDW is warming by about 0.01 °C/year and becoming more saline by 0.007/year.

In the central parts of the basins the differences in the water mass properties between southward- and northward-flowing waters are small. The water mass properties of northward and southward flows are averaged. Small-scale eddy motions can make waters with the same properties cross the strait in both directions, also since the

geostrophic velocities are computed between two hydrographic stations and the same temperature and salinity properties are combined with two different velocities on both sides of a CTD station (**Fig. 6**).

6.3 Volume transports of different water masses

The observed net outflow from the Arctic Ocean through the Fram Strait occurs mainly as low salinity and cold surface water, mostly over the Greenland continental slope, and as dAW and intermediate waters. The estimated net volume transport on the Greenland continental shelf varies from 0.1 to 1.0 Sv southward, partly due to the varying length of the sections, and consists mainly of surface water, and some AW. The cold and low salinity surface water carried by the EGC continues southward through the Fram Strait and is also found at the southern Greenland Sea section (paper V). The net volume transport of surface water through both the Fram Strait and Greenland Sea sections are of about equal size, 0.6-0.7 Sv southward.

The northward flow of AW in the eastern parts of the sections is larger than the southward flow of the cooler AW. In paper V the net volume transport of AW is estimated at 0.9 Sv (0.5-1.8 Sv) northward through the whole width of the 75 °N section and 0.7 Sv northward (0.0-1.3 Sv) through the Fram Strait section. In the earlier papers the net AW volume transport is estimated at about 0.1 Sv northward with large variability. About 1.4 Sv AW and dAW are estimated to flow northward past the section north of the Fram Strait in 2002 (paper II). The net volume transports of dAW are about 0.5-1.0 Sv southward through each of the three section locations.

The net intermediate water transports are southward and for 1999-2010 about 0.5 Sv. For the 1980-2005 time series the net volume transport varies between 0.6 to 1.4 Sv southward being about twice as large as that obtained from the quasi-closed boxes in 1999-2010 for the overlapping years 1999-2005. The net outflow of the intermediate water derives largely from the Barents Sea branch that enters the Arctic Ocean via the St. Anna Trough, also some of the southward flowing AW is deriving from the Barents Sea branch. The northward transport of AIW originating in the Nordic Seas is estimated from 2002 Oden data when excess SF_6 is available and can be used to distinguish AIW from the uPDW originating in the Arctic Ocean. It is estimated from geostrophic computations that 0.8 Sv intermediate water enters the Arctic Ocean across the section, of which 70% is AIW based on SF_6 concentrations; i.e. 0.5 Sv of AIW would enter the Arctic Ocean.

The bifurcation of the Fram Strait branch at intermediate depths is observed as positive excess SF_6 concentrations, deriving from the mixing experiment in the Greenland Sea, as it flows toward the Arctic Ocean. One branch follows the Yermak Plateau along its western flank and the other branch flows northward close to Svalbard (Rudels et al., 2000). Both of these branches are assumed to meet north of Svalbard and enter the Arctic Ocean (paper II, Figure 1), but whether the western branch northwest of the Yermak Plateau first branches off with part of it following the slopes around the Sofia Deep, as suggested in paper II, has not received significant support.

CBDW flows southward in the western part of the Fram Strait, both over the slope and the deep basin. EBDW flows southward in the deep basins, but some recirculation of it is also observed as a northward flow in the eastern deep basin. NDW flows in both directions in the Fram Strait. On the Svalbard slope and in the deep basins its northward flow is larger than the southward. The deep transports in paper I are constrained with constant volume and salt transports. These volume transports are also

computed from the newer estimates, and the use of 0.4 Sv southward as a deep constraint seems reasonable (**Table 4**). The net volume transports of the deep waters are small, partly due to the step-wise bottom topography and the choice of setting the initial velocities to zero near bottom.

The exchange rate of the deep waters between the Fram Strait and the Greenland Sea has remained fairly constant over 1999-2010.

6.4 Recirculation

Besides the strong currents on both sides of the Fram Strait, WSC to the east and EGC to the west, a substantial amount of recirculation takes place in the strait. Narrow barotropic and baroclinic eddies have been found to drift westward along the Fram Strait sill (e.g. Teigen et al., 2011).

The recirculation in the Fram Strait is estimated in paper IV: firstly from two zonal sections, as northward volume transport through the 79 °N section minus northward volume transport through the northern section attaining 2 Sv for the Atlantic waters, and secondly through a meridional section across the Greenwich meridian reaching from 78 °N to 80 °N resulting in somewhat less.

The westward circulation in the Fram Strait can also be observed from the drift of the Argo floats with 1000 dbar parking depth (paper V, Figure 2). The Argo data located in the vicinity of the Fram Strait are still sparse. Based mainly on the meridional sections in paper IV, the recirculation in the Fram Strait is estimated to be strongest close to the 79 °N latitude.

This work as well as previous and later studies (Bourke et al., 1988; Rudels, 1987; Manley, 1995; de Steur et al., 2014) result in the same estimate that about half of the northward-flowing AW in the Fram Strait recirculates back to the south.

6.5 Heat transports

About one quarter of the Arctic Ocean's heat flux is carried through the Fram Strait as estimated by Tsubouchi et al. (2012). The heat transport through the Fram Strait derives mostly from the warm and saline AW and is in paper I estimated as 25 TW northward using a varying reference temperature. The mean of the varying reference temperatures, as the average temperature of the flow out of the Arctic Ocean through the strait from the observations 1980-2005, is about 0.7 °C. Using the commonly used reference temperature -0.1 °C the heat transport reduces to 17 TW. The value obtained from current meter moorings is about 40 TW during the study period (Schauer et al., 2004) and somewhat less using a stream tube concept to avoid the arbitrary nature of the results obtained through an unbalanced section (Schauer and Beszczynska-Möller, 2009).

In papers IV and V quasi-closed boxes are formed and the heat loss in areas closed by CTD sections to the north and south and continental shelf slopes to the east and west is estimated. The results are nearly independent of the reference values. The heat loss from the more southern of these two areas, between the Greenland Sea section and the Fram Strait section, is estimated at 9 ± 12 TW from 1999-2010 data. From the area north of the Fram Strait the heat loss as averaged over 3-4 years between 1984 and 2004 is estimated at about 11 TW.

6.6 Freshwater transports

The freshwater is carried out of the Arctic Ocean in roughly equal parts of ice and liquid water (Carmack et al., 2015). Most of the ice and almost half of the liquid freshwater exits the Arctic Ocean via the Fram Strait (Aagaard and Carmack, 1989; Dickson et al., 2007; Tsubouchi et al., 2012). In this work the liquid freshwater transports are estimated.

The liquid freshwater transports through the Fram Strait occur mostly in the surface layer and are mainly due to ice melt, river runoff and water diluted by these inputs exiting the Arctic Ocean. Freshwater export as sea ice is about 70-100 mSv (Vinje, 2001; Kwok et al., 2004; Carmack et al., 2015). In paper I the freshwater transport through to the Fram Strait is estimated as 30-50 mSv southward between 6 °W and 9 °E, and as 0.65 mSv when the transport across the Greenland continental shelf is included. A significant amount of the freshwater transport takes place over the Greenland shelf and is often lacking from the results in paper I due to varying section lengths, and to the stations only covering part of the shelf (**Fig. 8**). The freshwater transport is less sensitive to the reference value than heat transport.

The freshwater transports are also estimated in papers IV and V using a reference salinity 34.9 (V), 34.8 (IV) and a mean salinity from the sections forming the quasi-closed box (IV). The freshwater transports obtained in paper IV are below 60 mSv through the 79 °N section and about 20 mSv through the northern section, implying that about 40 mSv of the freshwater input between the sections in the summertime would be mainly due to ice melt. The precipitation in the area contributes to a small degree. The freshwater transports through the Fram Strait section are in paper V estimated at 66 ± 9 mSv and through the 75 °N section at 54 ± 20 mSv. This Fram Strait value is somewhat smaller than the less than 100 mSv value estimated by e.g. Carmack et al. (2015).

7 Conclusions

7.1 Volume transports

The net volume transports through the Fram Strait estimated in this work based on hydrography with varying sets of constraints applied range from 4.6 Sv to the south in 1998 with constraints set on the deep waters (paper I) to 2.4 Sv northward from quasi-closed boxes between the Fram Strait and the Greenland Sea and using the velocity information from the Argo floats in 2001 (paper V, Fig. 3). The net volume transports averaged for 1980-2005 are 2.5 Sv + 0.3 Sv southward (paper I), or 1.7 Sv from budget considerations, 3.1 Sv southward averaged from 4 years of data from quasi-closed boxes between 1984-2004 (paper IV) and 0.8 ± 1.5 Sv southward for 1999-2010 (paper V) (**Fig. 10**). The net volume transports in the Fram Strait have been continuously monitored from current meter moorings since 1997. The transports are highly variable, albeit with a decrease in variability since 2001 when the mooring location was moved from 79 °N to 78 °50 'N (de Steur et al., 2014). The northward and southward volume transports (monthly means) vary between slightly over 5 Sv to over 20 Sv in both directions and the net volume for 1997-2005 is 1.75 ± 5.01 Sv (Fieg et al., 2010), and for 1999-2010 2.8 ± 3.5 Sv (Schauer and Beszczynska-Möller, 2009, extended timeseries). Although a seasonal signal is present in the WSC with a wintertime maximum (e.g. Fahrbach et al., 2001; Schauer et al., 2004) and in the EGC at 78 °50 'N with a winter maximum and summer minimum (de Steur et al., 2014) no clear seasonal signal is found in the net volume transports except between 2002-2005 (Schauer and Beszczynska-Möller, 2009, Fig. 5). The estimates presented in this work for the volume transports agree well with those obtained from the current meter moorings and from models (e.g. Fieg et al., 2010), both for the net and individual northward and southward volume transports, partly due to the large variability in the mooring results. The mean volume transports based on geostrophic estimates are smaller than the mean volume transports estimated from the current meter moorings. The results based on hydrographic data offer summertime snapshots and add to the ensemble of estimates for the Fram Strait transports. However, aliasing can occur especially during the earlier years of data due to sparse station spacing that allows baroclinic and barotropic eddies present in the Fram Strait to evade detection. The Ekman transport is largely ignored in this work; in paper IV its effect on the net surface flow is estimated to be small in the Fram Strait during the time of observations due to a varying wind field.

The smallest net volume transports of 0.8 Sv southward are estimated in paper V using a linear fit to the Argo data. The small net volume is partly due to having one year with high net northward transport; excluding that year, the net transports would be 1.2 Sv southward. This is better in agreement with other estimates, but still low (**Fig. 10**). Without the Argo adjustment the transports are 1.9 Sv southward, but the AW transport reduces from 0.7-0.8 Sv northward to 0.1 Sv northward. Since the AW, having entered the Arctic Ocean also through the Barents Sea, mostly returns through the Fram Strait, determining which estimate is better would require a more thorough investigation of the water mass transformations than is presented in this work, including not just the surface water, containing diluted AW, the colder and deeper lying dAW, but also some of the intermediate and even deep waters formed in the Arctic Ocean through cascading of dense shelf waters. However, the net volume transports obtained in this work for the Fram Strait can be judged against volume transport estimates for the other entrances to

the Arctic Ocean (**Fig. 5**). Taking the given error margins and variance in the given transport estimates through the other passages, net volume transport through the Fram Strait could vary between 0.95 and 3.2 Sv southward and the Arctic Ocean volume budget could still be balanced.

The transports are in this work estimated from hydrographic data using the geostrophic method. LADCP data have been used to estimate the transports north of the Fram Strait in 2002 and vessel mounted ADCP in 2004. The use of CTD stations for estimating the transports instead of current meter moorings in the Fram Strait where an array of current meter moorings has been maintained regularly since 1997 is justified with their finer spatial resolution than that of current meter moorings. The temporal resolution with cruises mainly from the summertime is much worse. The geostrophic method cannot determine the barotropic transports, something that in this work is compensated for by not allowing the slope currents to flow in a direction other than that shown by the current meter moorings (all papers), and by using velocities obtained from the Argo floats to adjust the geostrophic velocities (paper V). Using ADCP velocities as a level of known motion for the geostrophic velocities has its difficulties since the shape of the velocity profiles obtained through direct current measurements differs from that obtained through geostrophy, the current meters capturing shorter time scale events than geostrophy. The transports are in paper II computed both from the lADCP derived and geostrophic velocities, and the lADCP derived northward and southward transports are 3-4 times higher. Both methods have their shortcomings, e.g. geostrophy lacks a representation for the barotropic part and lADCP data contains short term fluctuations, making the observations not synoptic.

The Fram Strait branch can be seen bifurcating based on the location of the excess SF_6 data, supporting the existing view (e.g. Rudels et al., 2000) that some of it flows around the Yermak Plateau and some takes a straighter route into the Arctic Ocean.

7.2 Water masses

The Fram Strait is the only deep passage between the Arctic Ocean and the rest of the world's oceans. Water masses pass through it as well as recirculate in it. On the eastern side, WSC carries warm and saline AW; on the western side EGC carries cold and low-salinity surface water. The deep waters from the Nordic Seas are transported northward and the Arctic Ocean waters southward. They mix with the surrounding waters along their way to the Fram Strait, within the Fram Strait (von Appen et al., 2015), and after having passed through it.

The surface layer in the Fram Strait mainly consists of water from river runoff, ice melt and diluted AW, precipitation and occasionally Pacific water from the Bering Strait (e.g. Rabe et al., 2013). The properties are highly variable, both spatially across the strait and temporally, being also affected by climate change.

The northward-flowing AW varies in its properties and extent. There have been warm pulses in the past and a warming trend in the 2000s with a maximum in 2006 (Beszczynska-Möller et al., 2012, extended time series). The southward-flowing AW is less saline and cooler than the northward-flowing, as expected from cooling and mixing in the Arctic Mediterranean.

The AIW properties have changed, and AIW has become warmer and more saline at its origins in the Nordic Seas. Of the intermediate waters flowing northward

through the Fram Strait 70% was estimated as AIW based on the SF_6 concentrations, 0.5 Sv of AIW would then enter the Arctic Ocean.

The deep waters in the Arctic Ocean have ventilation times of up to several hundreds of years and while their temperatures during these 3 decades of observations have risen only slightly and salinities remained about the same, the deep waters in the Greenland Sea have undergone drastic changes and continue to become warmer and more saline as they interact with the Arctic Ocean derived deep waters, while the Greenland Sea convection hardly reaches 2000 dbar thus not ventilating the deep waters. The properties of Arctic Ocean- and Nordic Seas-derived deep waters have become similar. Future studies will show if and how this will affect the circulation patterns in the northern seas together with other factors e.g. expected increase in precipitation, but perhaps also in evaporation, and less sea ice.

7.3 Recirculation

The recirculation in the Fram Strait is estimated using zonal and meridional sections. About 2 Sv, approximately half of the AW reaching the Fram Strait is estimated to recirculate south-westward in the strait. Other studies are currently giving similar estimates for the recirculation based on e.g. moorings (de Steur et al., 2014).

7.4 Heat and freshwater transports

During the 1980-2005 observation period in paper I the salinities of the northward flow in the Fram Strait range between 34.8 and 35 and average at 34.92. The mean salinity of the southward flow is about 34.8. The freshwater transport relative to the inflow salinity ranges between 20 and 100 mSv with the mean at 40 ± 10 mSv. From the 1999-2010 time series, 66 mSv at the Fram Strait is obtained using a reference salinity of 34.9. The results are in the same range but lower than those by Rabe et al. (2013) or Carmack et al. (2015).

Freshwater is gained in the box north of the Fram Strait, but lost from the southern box between the Fram Strait and the Greenland Sea, with large variability.

The heat loss from both the area north of the Fram Strait and south of it, closed by CTD sections, was estimated at about 10 TW. This compares well with the estimate of heat loss of 12.7 TW by Cisewski et al. (2003) for 1997 between a section in the Fram Strait at 79 °40 'N and a section at 75 °N using a constant net volume of 1.6 Sv southward and ship mounted ADCPs to adjust geostrophic velocities.

7.5 Future needs

Reports of climatic changes taking place in the Arctic occur frequently in the news. Among them, release of methane, melting permafrost, melting sea ice, and changes in weather patterns give cause for alarm. The icy Arctic as we know it appears to be vanishing, leaving dark winters and light summers as a poor consolation. The Arctic feedback systems are difficult to study and even harder to predict due to their complex nature. New measurements are crucial in improving our understanding of the Arctic. The Arctic Ocean is becoming more easily accessible and improved observational instruments are being developed. In this work, in addition to ship-borne measurements and a traditional method of geostrophy, data from Argo floats are used to study the

circulation. The Argo floats are profiling floats that also provide information about temperature, salinity and possible additional parameters, providing year-round information. Most of them only make profiles to 2000 dbar, but they are being developed for deeper measurements too, and at present 10 of the nearly 4000 Argo floats drifting in the oceans are capable of performing deep profiles down to 6000 dbar. A combination of deeper measurements and the ability to collect measurements in ice-covered waters (or in an ice-free Arctic Ocean), could help bring such understanding.

For estimations at the Arctic Ocean budgets, all the water transport gateways need to be monitored densely and continuously over a longer period of time in order to capture data on how the variability at one entrance is reflected at another, and with what time lag. This could lead to a balanced picture of the Arctic's oceanographic system.

Modelling is needed to fill gaps in observational data and in making future predictions. Observations are needed to keep track of the changes taking place in the northern seas and to improve the model accuracy. Possibly there still are some discoveries to be made in the Arctic waters.

7.6 A short summary

The Fram Strait has been the subject of many studies. The results in this work contribute to these efforts. Transports estimated from double sections bring reliability to the obtained volume and freshwater transports and allow for estimating the heat loss from areas north and south of the Fram Strait. The recirculation of AW is found to be similar to that presented in the 1980s. The tracer SF_6 allows for distinguishing between AIW and uPDW in the Fram Strait and to estimate how much AIW is transported through the Fram Strait into the Arctic Ocean. During the study period the properties of water masses in the Fram Strait changed and the water mass definition was modified.

Acknowledgements

Many people have helped me during this process. A complete list would be too long to be presented here, and honestly, would probably never even get finished out of fear of forgetting someone from it. It has been a rather long journey after all.

First, I thank my supervisor Bert Rudels for his expertise, guidance and help with all the manuscripts, and especially for arranging me to join several research cruises in the Arctic and sub-Arctic seas in the realm of the polar bear and icebergs.

I thank the pre-examiners Pentti Mälkki and Kai Myrberg for their comments and critique on this manuscript. I thank Matti Leppäranta, who has lectured most of the oceanography and sea ice courses that I have taken, for being an inspiring figure throughout my studies.

I thank Tuomo Saloranta for first introducing me to physical oceanography, and Tari Oksanen for hinting me about a vacancy that became my first job in research in 1999. I thank Jari Haapala, my boss in 1999 and now the head of the Marine research unit in the Finnish Meteorological Institute, for his enthusiasm towards the oceans and world in general. I also warmly thank the co-workers and students at the geophysics department in Fabianinkatu 24 during 1999 for the cosy atmosphere.

I thank Patrick Eriksson and all my other co-authors for their valuable work, and also for the moral support they have given me while preparing the manuscripts.

I thank Timo Vihma and Roberta Pirazzini for their help with meteorology and other matters. I thank the personnel of the former Finnish Institute of Marine Research and my current colleagues at the Finnish Meteorological Institute for the many conversations and cheerful lunch company.

I thank the captains, crews, cruise leaders and participants to the cruises on RV Aranda and on the other research vessels. I thank Riikka Hietala and Tero Purokoski for teaching me all I ever needed to know about CTD measurements. I thank Alf Norkko for his comments regarding paper IV during a cruise in the Baltic Sea, the conversations with Jinping Zhao during the IPY cruise on MV XueLong, and the other people for the good times and their patience.

I thank Anna Petelin Uotila for the language revision. I thank Petteri Uotila for helping me with NEMO, in my attempt to explore what sort of research possibilities there could be after the thesis.

This work was funded by the EU programs ASOF and DAMOCLES, the Academy of Finland, and the Väisälä Foundation. I also acknowledge the Kilpisjärvi biological station which for a reasonable price provided a beautiful and peaceful setting for finalising paper V before the initial submission.

The final thanks go to cat sitters, friends and relatives who have made it possible for me to cruise around the Arctic, and then shared fun, and less fun, moments with me on dryish land.

References

Aagaard, K. (1981). On the deep circulation in the Arctic Ocean, Deep Sea Research, 28, 251-268, doi:10.1016/0198-0149(81)90066-2.

Aagaard, K., and E. Carmack (1989). The role of sea ice and other fresh water in the Arctic circulation, Journal of Geophysical Research, 94(C10), 14485-14498, doi:10.1029/JC094iC10p14485.

Aagaard, K., C. Darnall, and P. Greisman (1973). Year-long current measurements in the Greenland-Spitsbergen passage, Deep Sea Research, 20(8), 743-746, doi:10.1016/0011-7471(73)90090-9.

Aagaard, K., and P. Greisman (1975). Toward new mass and heat budgets for the Arctic Ocean, Journal of Geophysical Research, 80(27), 3821-3827.

Aagaard, K., J. H. Swift, and E. C. Carmack (1985). Thermohaline circulation in the Arctic Mediterranean Seas, Journal of Geophysical Research, 90(C3), 4833-4846, doi:10.1029/JC090iC03p04833.

Arrigo, K. R., G. van Dijken, and S. Pabi (2008). Impact of a shrinking Arctic ice cover on marine primary production, Geophysical Research Letters, 35, L19603, doi:10.1029/2008GL035028.

Berx, B., B. Hansen, S. Østerhus, K. M. Larsen, T. Sherwin, and K. Jochumsen (2013). Combining in situ measurements and altimetry to estimate volume, heat and salt transport variability through the Faroe–Shetland Channel, Ocean Science, 9(4), 639-654, doi:10.5194/os-9-639-2013.

Beszczynska-Möller, A., E. Fahrbach, U. Schauer, and E. Hansen (2012). Variability in Atlantic water temperature and transport at the entrance to the Arctic Ocean, 1997–2010, ICES Journal of Marine Science, 69, 852–863, doi:10.1093/icesjms/fss056.

Bourke, R. H., A. M. Weigel, and R. G. Paquette (1988). The westward turning branch of the West Spitsbergen Current, Journal of Geophysical Research, 93(C11), 14065–14077, doi:10.1029/JC093iC11p14065.

Bromaghin, J. F., T. L. McDonald, I. Stirling, A. E. Derocher, E. S. Richardson, E. V. Regehr, D. C. Douglas, G. M. Durner, T. Atwood, and S. C. Amstrup (2015). Polar bear population dynamics in the southern Beaufort Sea during a period of sea ice decline, Ecological Applications, 25, 634-651, doi:10.1890/14-1129.1.

Budéus, G., W. Schneider, and G. Krause (1998). Winter convective events and bottom water warming in the Greenland Sea, Journal of Geophysical Research, 103(C9), 18513-18527.

Bönisch, G., and P. Schlosser (1995). Deep water formation and exchange rates in the Greenland / Norwegian Seas and the Eurasian Basin of the Arctic Ocean derived from tracer balances, Progress in Oceanography, 35(1), 29-52.

Carmack, E. 1, M. Yamamoto-Kawai, T. Haine, S. Bacon, B. Bluhm, C. Lique, H. Melling, I. Polyakov, F. Straneo, M.-L. Timmermans, and W. Williams (2015). Freshwater and its role in the Arctic Marine System: Sources, disposition, storage, export, and physical and biogeochemical consequences in the Arctic and global oceans, Journal of Geophysical Research: Biogeosciences, 121, 675-717, doi: 10.1002/2015JG003140.

Cisewski, B., G. Budéus, and G. Krause (2003). Absolute transport estimates of total and individual water masses in the northern Greenland Sea derived from hydrographic and acoustic Doppler current profiler measurements, Journal of Geophysical Research: Oceans, 108(C9), 3298, doi:10.1029/2002JC001530.

Coachman, L. K., and C. A. Barnes (1963). The movement of Atlantic water in the Arctic Ocean, Arctic, 16(1), 8-16.

Curry, B., C. M. Lee, B. Petrie, R. E. Moritz, and R. Kwok (2014). Multiyear volume, liquid freshwater, and sea ice transports through Davis Strait, 2004–10*, Journal of Physical Oceanography, 44(4), 1244–1266, doi: http://dx.doi.org/10.1175/JPO-D-13-0177.1.

de Steur, L., E. Hansen, C. Mauritzen, A. Beszczynska-Möller, and E. Fahrbach (2014). Impact of recirculation on the East Greenland Current in Fram Strait: Results from moored current meter measurements between 1997 and 2009, Deep Sea Research, 92, 26-40, doi:10.1016/j.dsr.2014.05.018.

Dickson, R., B. Rudels, S. Dye, M. Karcher, J. Meincke, and I. Yashayev (2007). Current estimates of freshwater flux through Arctic and subarctic seas, Progress in Oceanography, 73(3), 210-230, doi:10.1016/j.pocean.2006.12.003.

Dickson, B., S. Dye, S. Jónsson, A. Köhl, A. Macrander, M. Marnela, J. Meincke, S. Olsen, B. Rudels, H. Valdimarsson, and G. Voet (2008). The overflow flux west of Iceland: Variability, origins and forcing. In: B. Dickson, J. Meincke & P. Rhines (Eds.), Arctic-Subarctic Ocean Fluxes: Defining the role of the Northern Seas in Climate, Springer, Dordrecht, 443–474.

Dmitrenko, I. A., B. Rudels, S. A. Kirillov, Y. O. Aksenov, V. S. Lien, V. V. Ivanov, U. Schauer, I. V. Polyakov, A. Coward, and D. G. Barber (2015). Atlantic water flow into the Arctic Ocean

through the St. Anna Trough in the northern Kara Sea, Journal of Geophysical Research: Oceans, 120(7), 5158-5178, doi:10.1002/2015JC010804.
Emery, W. J. and J. Meincke (1986). Global water masses: Summary and review, Oceanologica Acta, 9(4), 383-391.
Fahrbach, E., J. Meincke, S. Østerhus, G. Rohardt, U. Schauer, V. Tverberg, and J. Verduin (2001). Direct measurements of volume transports through Fram Strait. Polar Research, 20(2), 217–224.
Falck, E., G. Kattner, and G. Budéus (2005). Disappearance of Pacific water in the northwestern Fram Strait, Geophysical Research Letters, 32, L14619, doi:10.1029/2005GL023400.
Fieg, K., R. Gerdes, E. Fahrbach, A. Beszczynska-Möller, and U. Schauer (2010). Simulation of oceanic volume transports through Fram Strait 1995–2005, Ocean Dynamics, 60(3), 491–502, doi:10.1007/s10236-010-0263-9.
Foldvik, A., K. Aagaard, and T. Tørresen (1988). On the velocity field of the East Greenland Current, Deep Sea Research, 35(8), 1335-1354, doi:10.1016/0198-0149(88)90086-6.
Hansen, B., K. M. H. Larsen, H. Hátún, R. Kristiansen, E. Mortensen, and S. Østerhus (2015). Transport of volume, heat, and salt towards the Arctic in the Faroe Current 1993-2013, Ocean Science, 11(5), 743-757, doi:10.5194/os-11-743-2015.
Helland-Hansen, B. (1918). Nogen hydrografiske metoder (Some hydrographic methods), Forhandlinger ved de Skandinaviske Naturforskeres 16de møte (juli 1916), Kristiania, 357-359. (In Norwegian).
Holland, M., D. A. Bailey, B. P. Briegleb, B. Light, and E. Hunke (2012). Improved sea ice shortwave radiation physics in CCSM4: The impact of melt ponds and aerosols on Arctic sea ice, Journal of Climate, 25(5), 1413-1430, doi:10.1175/JCLI-D-11-00078.1.
Houssais, M.-N., B. Rudels, H. Friedrich, and D. Quadfasel (1995). Exchanges through Fram Strait, in: Nordic Seas Symposium on the Results of the Greenland Sea Project (GSP) 1987–1993, Extended Abstracts, edited by: Meincke, J., US National Science Foundation, Hamburg, 87–91.
Ingvaldsen, R. B., L. Asplin, and H. Loeng (2004). Velocity field of the western entrance to the Barents Sea, Journal of Geophysical Research, 109, C03021, doi:10.1029/2003JC001811.
Jacobsen, J. P., and A. J. C. Jensen (1926). Examination of hydrographic measurements from the research vessels Explorer and Dana during the summer of 1924, Conseil Permanent International pour l'Exploration de la Mer, Rapports et Procès-Verbaux, 39, 31–84.
Jakobsson, M., L. Mayer, B. Coakley, J. A. Dowdeswell, S. Forbes, B. Fridman, H. Hodnesdal, R. Noormets, R. Pedersen, M. Rebesco, and H. W. Schenke (2012). The International Bathymetric Chart of the Arctic Ocean (IBCAO) version 3.0, Geophysical Research Letters, 39, L12609, doi:10.1029/2012GL052219.
Jones, E. P., and L. G. Anderson (1986). On the origin of the chemical properties of the Arctic Ocean halocline, Journal of Geophysical Research, 91(C9), 10759-10767.
Jones, E. P., and L. G. Anderson (2008). Is the Global Conveyor Belt Threatened by Arctic Ocean Fresh Water Outflow?, In: Dickson, R. R., J. Meincke and P. Rhines (Eds.) Arctic-Subarctic Ocean Fluxes, Springer, Dordrecht, 385-404.
Jónsson, S., and H. Valdimarsson (2012). Water mass transport variability to the North Icelandic shelf, 1994–2010, ICES Journal of Marine Science, 69, 809–815, doi:10.1093/icesjms/fss024.
Karcher, M. J., and J. M. Oberhuber (2002). Pathways and modification of the upper and intermediate waters of the Arctic Ocean, Journal of Geophysical Research, 107(C6), doi:10.1029/2000JC000530.
Karcher, M., J. N Smith, F. Kauker, R. Gerdes, and W. M Smethie Jr. (2012). Recent changes in Arctic Ocean circulation revealed by iodine-129 observations and modeling, Journal of Geophysical Research, 117, C08007, doi:10.1029/2011JC007513.
Kwok, R., G. F. Cunningham, and S. S. Pang (2004). Fram Strait sea ice outflow, Journal of Geophysical Research: Oceans, 109, C01009, doi:10.1029/2003JC001785.
Kwok, R. (2009). Outflow of Arctic sea ice into the Greenland and Barents Seas: 1979-2007, Journal of Climate, 22(9), 2438-2457, doi: 10.1175/2008JCLI2819.1.
Lanczos, C. (1970). The variational principles of mechanics, 4th Edn., University of Toronto Press, Toronto, 418 pp.
Langehaug, H. R., and E. Falck (2012). Changes in the properties and distribution of the intermediate and deep waters in the Fram Strait, Progress in Oceanography, 96(1), 57-76, doi:10.1016/j.pocean.2011.10.002.
Losch, M., D. Sidorenko, and A. Beszczynska-Möller (2005). FEMSECT: An inverse section model based on the finite element method, Journal of Geophysical Research: Oceans, 110, C12023, doi:10.1029/2005JC002910.

Mamayev, O. I. (1975). Temperature-Salinity analysis of world ocean waters, Elsevier Scientific, Amsterdam-Oxford-New York, 374 pp.

Manley, T. O. (1995). Branching of Atlantic Water within the Greenland-Spitsbergen Passage: An estimate of recirculation, Journal of Geophysical Research, 100(C10), 20627–20634, doi:10.1029/95JC01251.

Nansen, F. (1902). Oceanography of the North Polar Basin, The Norwegian North Polar Expedition 1893-1896, Scientific Results (9), 427 pp.

Nummelin, A., C. Li, and L. H. Smedsrud (2015). Response of Arctic Ocean stratification to changing river runoff in a column model, Journal of Geophysical Research: Oceans, 120(4), 2655–2675, doi:10.1002/2014JC010571.

Orr, J. C., V. J. Fabry, O. Aumont, L. Bopp, S. C. Doney, R. A. Feely, A. Gnanadesikan, N. Gruber, A. Ishida, F. Joos, R. M. Key, K. Lindsay, E. Maier-Reimer, R. Matear, P. Monfray, A. Mouchet, R. G. Najjar, G.-K. Plattner, K. B. Rodgers, C. L. Sabine, J. L. Sarmiento, R. Schlitzer, R. D. Slater, I. J. Totterdell, M.-F. Weirig, Y. Yamanaka, and Andrew Yool (2005). Anthropogenic ocean acidification over the twenty-first century and its impact on calcifying organisms, Nature, 437(7059), 681-686, doi:10.1038/nature04095.

Overland, J. E., and M. Wang (2013). When will the summer Arctic be nearly sea ice free?, Geophysical Research Letters, 40(10), 2097–2101, doi:10.1002/grl.50316.

Padman, L., and S. Erofeeva (2004). A barotropic inverse tidal model for the Arctic Ocean, Geophysical Research Letters, 31, L02303, doi:10.1029/2003GL019003.

Pond, S., and G. L. Pickard (1983). Introductory Dynamical Oceanography, 2nd edition, Elsevier Butterworth-Heinemann, Oxford, reprinted with corrections 2003, 329 pp.

Proshutinsky, A., D. Dukhovskoy, M.-L. Timmermans, R. Krishfield, and J. L. Bamber (2015). Arctic circulation regimes, Phil. Trans. R. Soc., A 373(2052), 20140160, doi:10.1098/rsta.2014.0160.

Quadfasel, D., A. Sy, D. Wells, and A. Tunik (1991). Warming in the Arctic, Nature, 350-385.

Rabe, B., P. A. Dodd, E. Hansen, E. Falck, U. Schauer, A. Mackensen, A. Beszczynska-Möller, G. Kattner, E. J. Rohling, and K. Cox (2013). Liquid export of Arctic freshwater components through the Fram Strait 1998-2011, Ocean Science, 9(1), 91-109, doi:10.5194/os-9-91-2013.

Rabe, B., U. Schauer, A. Mackensen, M. Karcher, E. Hansen., and A. Beszczynska-Möller (2009). Freshwater components and transports in the Fram Strait – recent observations and changes since the late 1990s, Ocean Science, 5(3), 219–233, doi:10.5194/os-5-219-2009.

Rahmstorf, S. (2006). Thermohaline Ocean Circulation. In: Encyclopedia of Quaternary Sciences, Edited by S. A. Elias. Elsevier, Amsterdam.

Rudels, B. (1987). On the mass balance of the Polar Ocean, with special emphasis on the Fram Strait, Norsk Polarinstitutt Skrifter, 188, 53 pp.

Rudels, B., L. G. Anderson, and E. P. Jones (1996). Formation and evolution of the surface mixed layer and halocline of the Arctic Ocean, Journal of Geophysical Research, 101(C4), 8807-8821.

Rudels, B., G. Björk, J. Nilsson, P. Winsor, I. Lake, and C. Nohr, (2005). The interactions between waters from the Arctic Ocean and the Nordic Seas north of Fram Strait and along the East Greenland Current: results from the Arctic Ocean-02 Oden expedition, Journal of Marine Systems, **55**, 1-30, doi:10.1016/j.jmarsys.2004.06.008.

Rudels, B., H. J. Friedrich, D. Hainbucher, and G. Lohmann (1999). On the parameterisation of oceanic sensible heat loss to the atmosphere and to ice in an ice-covered mixed layer in winter, Deep-Sea Research II, 46(6), 1385-1425.

Rudels, B., E. P. Jones, L. G. Anderson, and G. Kattner (1994). On the intermediate depth waters of the Arctic Ocean. In: O. M. Johannessen, R. D. Muench, J. E. Overland (Editors), The Polar Oceans and their role in shaping the global environment, Geophysical Monograph 85, 33-46.

Rudels, B., E. P. Jones, U. Schauer, and P. Eriksson (2001). Two sources for the lower halocline in the Arctic Ocean, ICES CM, 195, 18 pp.

Rudels, B., E. P. Jones, U. Schauer, and P. Eriksson (2004). Atlantic sources of the Arctic Ocean surface and halocline waters, Polar Research, 23(2), 181-208.

Rudels, B., M. Korhonen, U. Schauer, S. Pisarev, B. Rabe, and A. Wisotzki (2015). Circulation and transformation of Atlantic water in the Eurasian Basin and the contribution of the Fram Strait inflow branch to the Arctic Ocean heat budget, Progress in Oceanography, 132, 128-152, doi:10.1016/j.pocean.2014.04.003.

Rudels, B., R. Meyer, E. Fahrbach, V. V. Ivanov, S. Østerhus, D. Quadfasel, U. Schauer, V. Tverberg, and R. A. Woodgate (2000). Water mass distribution in Fram Strait and over the Yermak Plateau in summer 1997, Annales Geophysicae, 18, 687-705.

Rudels, B., U. Schauer, G. Björk, M. Korhonen, S. Pisarev, B. Rabe, and A. Wisotzki (2013). Observations of water masses and circulation in the Eurasian Basin of the Arctic Ocean from the 1990s to the late 2000s, Ocean Science, 9(1), 147-169, doi:10.5194/os-9-147-2013.

Schauer, U., and A. Beszczynska-Möller (2009). Problems with estimation and interpretation of oceanic heat transport – conceptual remarks for the case of Fram Strait in the Arctic Ocean, Ocean Science, 5(4), 487-494, doi:10.5194/os-5-487-2009.

Schauer, U., E. Fahrbach, S. Østerhus, and G. Rohardt (2004). Arctic warming through the Fram Strait: Oceanic heat transport from 3 years of measurements, Journal of Geophysical Research, 109, C06026, doi:10.1029/2003JC001823.

Schlichtholz, P., and M.-N. Houssais (2002). An overview of the θ-S correlations in Fram Strait based on the MIZEX 84 data, Oceanologia, 44, 243–272.

Serreze, M. C., A. P. Barrett, A. G. Slater, R. A. Woodgate, K. Aagaard, R. B. Lammers, M. Steele, R. Moritz, M. Meredith, and C. M. Lee (2006). The large-scale freshwater cycle of the Arctic, Journal of Geophysical Research 111, C11010, doi:10.1029/2005JC003424.

Shakhova, N., I. Semiletov, I. Leifer, V. Sergienko, A. Salyuk, D. Kosmach, D. Chernykh, C. Stubbs, D. Nicolsky, V. Tumskoy, and Ö. Gustafsson (2014). Ebullition and storm-induced methane release from the East Siberian Arctic Shelf. Nature Geoscience, *7*(1), 64-70.

Skagseth, Ø., K. F. Drinkwater, and E. Terrile (2011). Wind- and buoyancy-induced transport of the Norwegian Coastal Current in the Barents Sea, Journal of Geophysical Research, 116, C08007, doi:10.1029/2011JC006996.

Skogseth. R., P. M. Haugan, and M. Jakobsson (2005). Watermass transformations in Storfjorden, Continental Shelf Research, 25(5), 667-695, doi:10.1016/j.csr.2004.10.005.

Smedsrud, L. H., I. Esau, R. B. Ingvaldsen, T. Eldevik, P. M. Haugan, C. Li, V. S. Lien, A. Olsen, A. M. Omar, O. H. Otterå, B. Risebrobakken, A. S. Sandø, V. A. Semenov, and S. A. Sorokina (2013). The role of the Barents Sea in the Arctic climate system, Reviews of Geophysics, 51(3), 415-449, doi:10.1002/rog.20017.

Somavilla, R., U. Schauer, and G. Budéus (2013). Increasing amount of Arctic Ocean deep waters in the Greenland Sea, Geophysical Research Letters, 40(16), 4361-4366, doi:10.1002/grl.50775.

Srokosz, M., M. Baringer, H. Bryden, S. Cunningham, T. Delworth, S. Lozier, J. Marotzke, and R. Sutton (2012). Past, Present, and Future Changes in the Atlantic Meridional Overturning Circulation. Bulletin of the American Meteorological Society, 93(11), 1663–1676, doi: http://dx.doi.org/10.1175/BAMS-D-11-00151.1.

Spall, M. A. (2013). On the Circulation of Atlantic Water in the Arctic Ocean. Journal of Physical Oceanography, 43(11), 2352–2371, doi: http://dx.doi.org/10.1175/JPO-D-13-079.1.

Stephenson, S. R., L. C. Smith, L. W. Brigham, J. A. Agnew (2013). Projected 21st-century changes to Arctic marine access, Climatic Change, 118, 885–899, doi: 10.1007/s10584-012-0685-0.

Stommel, H. and G. Veronis (1981). Variational inverse method for study of ocean circulation, Deep Sea Research, 28(10), 1147–1160.

Stroeve, J. C., T. Markus, L. Boisvert, J. Miller, and A. Barrett (2014). Changes in Arctic melt season and implications for sea ice loss, Geophysical Research Letters, 41(4), 1216–1225, doi:10.1002/2013GL058951.

Sverdrup, H. U., M. W. Johnson, and R. H. Fleming (1942). The Oceans: Their physics, chemistry, and general biology. New York: Prentice-Hall, 1049 pp. http://ark.cdlib.org/ark:/13030/kt167nb66r/

Swift, J., and K. Aagaard (1981). Seasonal transitions and water mass formation in the Iceland and Greenland seas, Deep Sea Research, 28(10), 1107-1129, doi: 10.1016/0198-0149(81)90050-9.

Tanhua, T., E. P. Jones, E. Jeansson, S. Jutterström, W. M. Smethie Jr., D. W. R. Wallace, and L. G. Anderson (2009). Ventilation of the Arctic Ocean: Mean ages and inventories of anthropogenic CO_2 and CFC-11, Journal of Geophysical Research, 114, C01002, doi:10.1029/2008JC004868.

Teigen, S. H., F. Nilsen, R. Skogseth, B. Gjevik, and A. Beszczynska-Möller (2011), Baroclinic instability in the West Spitsbergen Current. Journal of Geophysical Research, 116, C07012, doi:10.1029/2011JC006974.

Tetzlaff, A., C. Lüpkes, G. Birnbaum, J. Hartmann, T. Nygård, and T. Vihma (2014). Brief Communication: Trends in sea ice extent north of Svalbard and its impact on cold air outbreaks as observed in spring 2013, Cryosphere, 8(5), 1757-1762, doi:10.5194/tc-8-1757-2014.

Treshnikov, A.F., Y. G. Nikiforov, and N. I. Blinov (1977). Results of the oceanological investigations by the "North Pole" drifting stations, Polar Geography, 1(1), 22-40.

Tsubouchi, T., S. Bacon, A. C. Naveira Garabato, Y. Aksenov, S. W. Laxon, E. Fahrbach, A. Beszczynska-Möller, E. Hansen, C. M. Lee, and R. B. Ingvaldsen (2012). The Arctic Ocean in summer: A quasi-synoptic inverse estimate of boundary fluxes and water mass transformation, Journal of Geophysical Research, 117, C01024, doi:10.1029/2011JC007174.

Vinje, T. (2001). Fram Strait ice fluxes and atmospheric circulation: 1950-2000, Journal of Climate, 14(16), 3508-3517.

Voet, G., D. Quadfasel, K. A. Mork, and H. Søiland (2010). The mid-depth circulation of the Nordic Seas derived from profiling float observations, Tellus, A 62(4), 516-529. doi:10.1111/j.1600-0870.2010.00444.x.

von Appen, W.-J., U. Schauer, R. Somavilla, E. Bauerfeind, and A. Beszczynska-Möller (2015). Exchange of warming deep waters across Fram Strait, Deep Sea Research, 103, 86-100, doi:10.1016/j.dsr.2015.06.003.

Walczowski, W., J. Piechura, I. Goszczko, and P. Wieczorek (2012). Changes in Atlantic water properties: an important factor in the European Arctic marine climate, ICES Journal of Marine Science, 69(5), 864-869, doi:10.1093/icesjms/fss068.

Watson, A.J., M.-J Messias, E. Fogelqvist, K. A. Van Scoy, T. Johannessen, K. I. C. Oliver, D. P. Stevens, F. Rey, T. Tanhua, K. A. Olsson, F. Carse, K. Simonsen, J. R. Ledwell, E. Jensen, D. J. Cooper, J. A. Kruepke, and E. Guilyardi (1999). Mixing and convection in the Greenland Sea from a tracer-release experiment, Nature 401, 902–904.

Wiig, Ø, L. Bachmann, V. M. Janik, K. M. Kovacs, and C. Lydersen (2007). Spitsbergen bowhead whales revisited, Marine Mammal Science, 23(3), 688-693, doi:10.1111/j.1748-7692.2007.02373.x.

Woodgate R. A., K. Aagaard, and T. J. Weingartner (2005). Monthly temperature, salinity, and transport variability of the Bering Strait through flow, Geophysical Research Letters, 32, L04601, doi:10.1029/2004GL021880.

Woodgate, R. A., E. Fahrbach, and G. Rohardt (1999). Structure and transports of the East Greenland Current at 75°N from moored current meters, Journal of Geophysical Research, 104(C8), 18059-18072, doi:10.1029/1999JC900146.

Woodgate, R. A., T. J. Weingartner, and R. Lindsay (2012). Observed increases in Bering Strait oceanic fluxes from the Pacific to the Arctic from 2001 to 2011 and their impacts on the Arctic Ocean water column, Geophysical Research Letters, 39, L24603, doi:10.1029/2012GL054092.

Worthington, L. V. (1953), Oceanographic results of project Skijump I and Skijump II in the Polar Sea, 1951–1952, Eos Transactions AGU, 34(4), 543–551, doi:10.1029/TR034i004p00543.

Wunsch, C. (1978), The North Atlantic general circulation west of 50° W determined by inverse methods, Reviews of Geophysics, 16(4), 583–620.

Abbreviations

AAW = Arctic Atlantic water
ADCP = Acoustic Doppler Current Profiler
AIW = Arctic Intermediate Water
ASOF = Arctic-Subarctic Ocean Fluxes
AW = Atlantic water
BG = Beaufort Gyre
CAA = Canadian Arctic Archipelago
CB = Canadian Basin, also known as Amerasian Basin
CBDW = Canadian Basin deep water
CBL = Chukchi Borderland
CFC = chlorofluorocarbon
CTD = Conductivity, Temperature, Depth; an instrument measuring conductivity, temperature and pressure
DAMOCLES = Developing Arctic Modelling and Observing Capabilities for Long-term Environmental Studies
dAAW = dense Arctic Atlantic Water
dAW = dense Atlantic water
EB = Eurasian Basin
EBDW = Eurasian Basin deep water
EGC = East Greenland Current
FHS = Fury and Hecla Strait
FJL = Franz Josef Land
FS = Fram Strait
GSDW = Greenland Sea deep water
IAW = Intermediate Arctic Water
lADCP = lowered Acoustic Doppler Current Profiler
IPY = International Polar Year (2007-2009)
NCC = Norwegian Coastal Current
NDW = Nordic Seas Deep Water
NEMO = Nucleus for European Modelling of the Ocean
PSW = Polar Surface Water
SAT = St Anna Trough
SD = Sofia Deep
SF_6 = sulphur hexafluoride
TPD = Transpolar Drift
uPDW = upper Polar Deep Water
VEINS = Variability of Exchanges in the Northern Seas
WSC = West Spitsbergen Current
wSW = warm Surface Water
YP = Yermak Plateau
θS diagram = potential temperature and salinity diagram

Corrections

In paper I the following information is missing from Table 13.1: Year 2003, Vessel RV Lance, programme ASOF, 21 stations between 6 °W and 9 °E, and 12 stations on the shelf.

In paper IV the equations B1 are incorrect in the appendix B. The C_k should be removed or there should be "+" instead of" = -" for all of the constraints (1) – (6)